Letters in Applied NanoBioScience
Open-Access Journal (ISSN: 2284-6808)

Review
Volume 13, Issue 1, 2024, 13
https://doi.org/10.33263/LIANBS131.013

TiO_2 Supported in Polymethyl methacrylate (PMMA) Properties, Preparation, and Photocatalytic Activity for the Degradation of Synthetic Dyes

Khaled Chawraba [1,2] *, Fouad Damiri [3], Joumana Toufaily [1,2], Jacques Lalevee [4,5], Tayssir Hamieh [6]

[1] Laboratory of Materials, Catalysis, Environment, and Analytical Methods Laboratory (MCEMA), Faculty of Sciences, Lebanese University, Hadath, Lebanon
[2] LEADDER Laboratory, Faculty of Sciences and EDST, Lebanese University, Hariri Campus, Hadath, Beirut, Lebanon; joumana.toufaily@ul.edu.lb (J.T.);
[3] University Hassan II of Casablanca, Faculty of Sciences Ben M'Sick, Department of Chemistry, Laboratory of Biomolecules and Organic Synthesis (BioSynthO), Casablanca, Morocco; fouad.damiri@hotmail.fr (F.D.);
[4] CNRS, IS2M UMR 7361, University of Haute-Alsace, Mulhouse, France; Jacque.lalevee@uha.fr (J.L.);
[5] University of Strasbourg, Strasbourg, France
[6] Faculty of Science and Engineering, Maastricht University, P.O. Box 616, 6200 MD Maastricht, The Netherlands; tayssir.hamieh@ul.edu.lb (T.H.);
* Correspondence: khaled.chawraba@outlook.com (K.C.);

Scopus Author ID 57687563400
Received: 30.07.2022; Accepted: 26.08.2022; Published: 23.04.2023

Abstract: The immobilization of titanium dioxide (TiO_2), a prominent photo-catalyst, on various substrates has received a lot of interest over the last two decades since it avoids the need for costly post-treatment separation methods. Among the many substrates tested for supporting TiO_2 photo-catalysts, polymer substrate appears to be the most promising due to multiple advantages such as its flexible nature, low cost, chemical resistance, mechanical stability, low density, high durability, and ease of availability. The proximity of photo-catalysis and the support system significantly increased the transfer step between adsorption and the total oxidative decolorization process. A comparison of photodecolorization with many synthetic dyes was made, and it was found that the structural and surface features of the photo-catalyst influenced the photocatalytic activities. This review focuses on TiO_2-PMMA nanocomposites and thoroughly investigates the synthesis, photocatalytic activity, and reuse of TiO_2/PMMA photo-catalysts. Finally, the future study scope and commercialization problems of PMMA-supported TiO2 photo-catalysts in visible and/or solar light have been highlighted.

Keywords: TiO_2; polymethyl methacrylate; photo-catalysis; supported catalysis; water treatment.

© 2023 by the authors. This article is an open-access article distributed under the terms and conditions of the Creative Commons Attribution (CC BY) license (https://creativecommons.org/licenses/by/4.0/).

1. Introduction

In recent years, water pollution has become a big concern for the scientific community since industrial and agricultural effluents, including organic and inorganic contaminants, are regularly released into the water stream, posing a substantial hazard to human health [1,2].

According to the United Nations World Water Development Report, about 748 million people worldwide do not have the provision that industrial production would require pure drinking water and that water demand will increase by 400 percent by 2050 [3]. Over 3.2 million children die yearly in poorer countries due to contaminated drinking water and poor sanitation [4]. The intake of a wide range of organic and inorganic substances harms environmental health [5].

Clean water is critical for human health; nevertheless, current water treatment systems have significant limitations [6,7]. As a result, it is desirable to create innovative water treatment methods that are low-cost and high-efficiency.

Various common approaches for sewage purification have historically been employed, including natural aerobic treatment, flocculation, coagulation, adsorption, membrane separation, Fenton processing, and rainfall [8,9]. However, owing to many constraints, such as expensive chemical and operational expenses, sophisticated processes, complicated sludge development, difficulties in separation, and long process time, conventional methods aren't as successful in wastewater treatment. Membrane separation technologies have several drawbacks, such as a short lifespan and limited selectivity during adsorption, with less pollution transfer across stages [6,7,10,11]. As a result, modern water technology solutions are unquestionably required.

Recent research initiatives have concentrated on advanced oxidation processes (AOPs) as possible novel water treatment methods. For the mineralization of non-biodegradable organic molecules and elimination of water pathogens, AOPs rely on in situ creation of highly reactive transient species via a light or other types of energy [5,9,12,13]. Due to its great efficiency as a photo-catalyst for environmental pollution treatment and energy production, heterogeneous photo-catalysis utilizing semiconductor nanostructures semi-conductive TiO_2 has received much attention among AOPs. Many investigations on the application of TiO_2 have been conducted. However, due to its disadvantages of only responding to UV and being difficult to recycle, its practical applicability is restricted [14–22].

It has been used in photocatalytic oxidation and removal of organic molecules in water, owing to its significant benefits of cheap cost [22], strong photocatalytic activity, chemical stability, and so on [2,5,23–26].

Heterogeneous photo-catalysis is one of the most promising water treatment methods, particularly in removing organic materials [8, 27–32]. It has been demonstrated to be highly effective in the breakdown of organic pollutants and the disinfection of pathogenic bacteria. Furthermore, when compared to traditional water treatment technologies, heterogeneous photo-catalysis has the following advantages: (1) a broad spectrum of effectiveness against various contaminants; (2) ambient operating pressure and temperature; and (3) complete degradation of the parent pollutants and their intermediate products [33].

TiO_2 has recently been widely employed in numerous environmental protection applications, such as the removal of water and air contaminants [34,35], Hazardous waste treatment [36,37], sterilization [38], deodorization [39], and NOx removal [40], and in the energy area, dye-sensitized solar cells [41,42], hydrogen evaluation [43], and self-cleaning surfaces [37], anti-corrosion applications, photocatalytic lithography [35], pigments, catalysts, and chemical sensors, etc. [42].

Titanium dioxide (TiO_2) has attracted the most attention because of its inexpensive cost, strong catalytic activity under UV light, environmental friendliness, and good stability [44–49].

Because of their enormous surface-to-volume ratio, size, and shape-dependent optical, electrical, and catalytic properties, TiO_2 nanostructures have a high potential as highly efficient photo-catalysts [50]. Several approaches to fabricating titanium dioxide nanoparticles for developing suitable photocatalytic instruments for water purification are described in the literature [51–55]. TiO_2 nanostructures may be synthesized by various techniques, including

sol-gel methods, template-assisted methods, hydro/solvothermal approaches, and various chemical processes [56–58].

TiO_2 has long been used as a photo-catalyst for generating a succession of reductive and oxidative reactions on its surface. In reality, when exposed to UV light, some photo-generated holes and electrons react with H_2O and O_2 molecules bound to the semiconductor surface, producing very reactive oxygen species (ROS) susceptible to mineralizing contaminants [59–66].

Furthermore, the produced ROS has an antibacterial impact via an oxidative stress mechanism, with the hydroxyl radical being the primary cause of bacterium inactivation [67].

Nonetheless, TiO_2 photo-catalysts have a low quantum efficiency due to their restricted spectrum response range caused by their broad bandgap and high photoinduced charge recombination rate. Furthermore, photo-catalysts are often difficult to recycle, which might restrict their use in the disposal of industrial wastewater [45].

However, the TiO_2 photo-catalyst particles agglomerate easily and lose activity. Furthermore, it's recycling for recurrent use becomes complex and expensive. These shortage issues severely limit the widespread use of TiO_2 in photo-catalysis [27,68,69]. However, there are substantial restrictions on nanomaterials' applications in consideration of their impacts on humans and the environment due to their employment [70,71].

Recently, polymers combined with semiconductor particles have formed new composites with novel physical properties, such as electrical and optical properties, that may be employed in photocatalytic and photoelectrical applications [72].

Polymeric nanocomposites combine nanomaterial properties with polymer characteristics, such as better durability, flexible nature, chemical resistance, lightweight, mechanical stability, wide availability, and cheap cost [73–76].

Polymeric nanocomposites have gotten a lot of interest in recent years in various disciplines of science and industry because they combine mechanical properties such as flexibility and relatively easy processing of polymers with the capabilities of nanoparticles [73,75–79]. The use of polymers in conjunction with photocatalytic materials enables the use of nanomaterials for water purification [80,81].

The immobilization of nanostructures in polymers avoids the need for a separation step following water treatment and decreases ecotoxicity concerns [37,82–86].

Furthermore, these solutions reduce the problem of nanomaterial aggregation, which is a common occurrence [87].

Immobilization of TiO_2 on porous silica [88–90] and porous carbon [91,92], glass, glass beads, quartz, silica, activated charcoal, fiberglass cloth, zeolites, stainless steel, ceramics, fabrics, monolith, and polymer membranes [93] is a typical way to increase TiO_2's photocatalytic activity.

When TiO_2 nanoparticles are integrated into a polymer matrix, all of the properties of the pure matrix could modify depending on the characteristics of individual components, the form, size, and amounts of the filler, and the system morphology [94].

TiO_2 incorporation on a polymer, particularly a transparent support, has also been observed [27,95,96]. Polymers are often low-cost, lightweight, and readily produced substrates, making them ideal for immobilizing semiconductors for heterogeneous photocatalytic degradation [97].

Various ways for attaching TiO_2 nanoparticles to various polymers have been widely documented, including liquid phase deposition, a dip coating method, phosphonate coupling, chemical reduction, emulsion polymerization, and spreading [98–103].

PMMA is an amorphous structure, linear chain, cheap production cost, optically clear (transparent) thermoplastic that is commonly utilized as a substitute for inorganic glass due to its high impact strength, lightweight, shatter-resistant properties, and advantageous processing conditions. Climate resistance and resistance to abrasion are two outstanding qualities [97]. It is widely utilized in physics in fiber optics, optical sensors, LEDs, and other applications [104]. Other uses for PMMA include biological applications [97] and photo-catalysis [105].

There are various advantages to using PMMA as the substrate material. PMMA film is a non-porous solid that is affordable, stable at high temperatures, and has a high pH value. Furthermore, PMMA is inert in a neutral aqueous medium and does not hydrolyze when used [106,107].

In creating the nanocomposites, poly (methyl methacrylate) (PMMA) serves as a polymer support. PMMA is a typical thermoplastic polymer used in various applications due to its transmittance of visible light, mechanical characteristics, and environmental durability; it is also a cost-effective and hydrophobic polymer that may meet food and drinks. PMMA is a suitable support for reactive inorganic particles, and many metal oxide fillers have been shown to increase its characteristics [108,109]. The incorporation of TiO_2 into a PMMA matrix, in particular, drew a lot of interest since it improved the glass transition temperature and thermal properties of the composite materials [74,110–113]. However, there has been minimal focus on using PMMA-TiO_2 nanocomposites for water filtration. We believe this has a significant impact on water purification difficulties.

PMMA's global adoption has been hampered by drawbacks such as a lack of UV-light filters and heat sensitivity. Nonetheless, integrating select semiconductors may mitigate some of these disadvantages [114,115].

Polymer nanofibers have a large specific surface area, which leads to quantum efficiency, a nanoscale effect with extraordinarily high surface energy, surface reactivity, high thermal and electrical conductivity, and biodegradability. Polymer nanofibers are very interesting for various applications, including catalyst supports, drug delivery systems, photonics, and sensors [116–119]. The resultant composites are easily removed from the solution and can be recycled [120].

Electrospinning is a one-of-a-kind technology for producing nanofibers using an electrically charged jet of the polymer solution [121–123]. Electrospinning may create pure polymer nanofibers, composite [124], and mixed [125,126] nanofibers. The electrical properties [124], surface hydrophobicity [126], and thermal properties [125,126] of a pure nanofiber can be improved by electrospinning a polymer matrix with functional fillers or another polymer matrix [127,128].

2. Synthetic Dyes

A dye is a colored and hazardous material that, when applied to clothes, provides a permanent color that is not eliminated by washing with water, detergents, or exposure to light. It is colored because it absorbs light in the entire visible spectrum at a specific wavelength [139–132].

Synthetic dyes are organic chemicals generated from benzene and its derivatives, such as methylene blue, eosin, Cristal violet, methylene orange, and fluorescein.

Synthetic dyes are substances with color that absorb light in the visible range (400–700 nm), including at least one chromophore as a color-bearing group, have a conjugated system as a structure with alternating double and single bonds, and display electron resonance [133]. All of these characteristics are required for synthetic dyes to have coloring qualities.

2.1. Categories, properties, and sources.

The first synthetic dyes were produced in 1856, starting with mauve dye (aniline), a gorgeous fuchsia color synthesized by W.H. Perkin (UK), and several azo dyes synthesized by diazotization reaction discovered by P. Gries in 1958. (Germany) [134].

Over 10,000 dyes are manufactured annually and used in various applications ranging from clothing to paper, food to wood, medicine, paint, chemistry, pharmaceuticals, leather, plastics, printing ink, rubber, cosmetics, and so on. It is almost entirely composed of synthetic materials, such as earth minerals and petroleum byproducts [32,129,132,135]. Previously, synthetic dyes were employed in garment finishes to create wrinkle-free, stain-resistant, flame-retardant, antistatic, antifungal, anti-bacterial, and odor-resistant fabrics that did not shrink. They can also be used as softening agents in other low-maintenance treatments [135].

Most synthetic dyes are less expensive to create, brighter, color faster, and easier to apply to fabrics. As a result, most research efforts focus on developing and formulating beautiful new colors, rendering natural dyes useless for most purposes [135].

These dyes are aromatic compounds derived via chemical synthesis, with aromatic rings containing undepleted electrons and various functional groups. The chromogen chromophore structure (acceptor of electrons) is responsible for their color, while auxochrome groups are responsible for their dyeing capacity (donor of electrons). The chromogen is made up of an aromatic structure that is often based on rings of benzene, naphthaline, or anthracene, from which binding chromophores with double conjugated links with dislocated electrons are formed. The azo function (-N=N-), ethylene function (=C=C=), methine function (-CH=), carbonyl function (=C=O), carbon-nitrogen (=C=NH; -CH=N-), carbon-sulfur (=C=S; C-S-S-C), nitro (-NO_2; -NO-OH), and nitroso (-N=O; =N-OH) serve as chromophore. The auxochrome groups are ionizable groups that provide colors that can attach to textile materials. -NH_2 (amino), -COOH (carboxyl), -SO_3H (sulphonate), and -OH are the most common auxochrome groups (hydroxyl) [131,134].

Meanwhile, auxochrome structures in chromophores such as carboxylic acid, sulfonic acid, amino, and hydroxyl groups function as color helpers to increase dye solubility [136].

Table 1 shows the characteristics (type, structure, and maximal absorption wavelength of some synthetic dyes.

Table 1. Four examples of textile dyes are presented.

Dyes	Type	λ_{max} (nm)	Molecular weight(g/mol)	Structure
Methylene blue	cationic	660	319.85	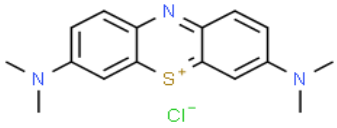

Dyes	Type	λ_{max} (nm)	Molecular weight(g/mol)	Structure
Rhodamine B	cationic	550	479.2	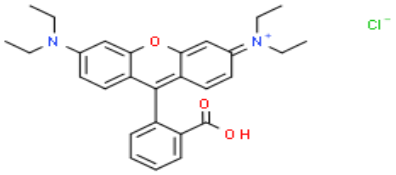
Crystal violet	cationic	590	407.99	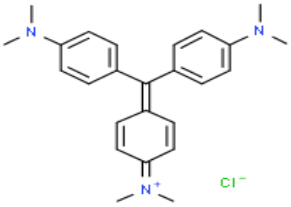
Reactive orange 16	anionic	495	617.54	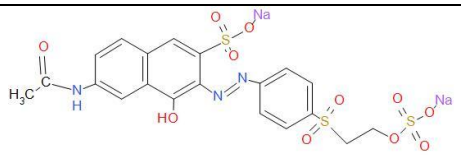

In general, the classification of dyes and other colored materials is based on the chemical characteristics responsible for their visibility and is generally consistent with the works of modern color scientists. Because of the difficulties of the chemical structure system's color nomenclature, the classification in terms of application is frequently desirable. Their chemical structures determine the colors, qualities, and uses of dyes, which are the only plausible basis for dye classification. Dyes can be classed in various ways, including color, functional groups of molecules, and application methods [137,138].

Aside from that, dyes are typically classed based on their particle charge following dissolving in an aqueous application media, such as cationic dyes, which include basic dyes, and anionic dyes, which include direct, acid, and reactive dyes, and non-ionic dyes (dispersed dyes) [139–141].

azo dyes, Acid dyes, basic dyes, direct dyes, naphtha dyes, reactive dyes, mordant dyes, vat dyes, disperse dyes, and sulfur dyes [142] are the most often used dyes in the textile industry, with azo derivatives-based dyes being the most widely employed.

Textile dyes are divided into anionic, nonionic, and cationic dyes based only on their general structure. The principal anionic dyes are direct, acid, and reactive dyes [143], with the highly colored, the most dangerous dye they water-soluble reactive and acid dyes because they are not eliminated through the traditional treatment process. The principal nonionic dyes are dispersed dyes that do not ionize in water, and the major cationic dyes are azo basic, anthraquinone disperses, and reactive dyes, among others.

2.2. Effect on environments, human and aquatic lives.

Many colors used in many industries are poisonous and carcinogenic, posing a major threat to aquatic living beings. The toxicity and impact of dyes released into the environment via wastewater have thus been thoroughly researched [144,145].

The most dangerous colors are those derived from recognized carcinogens like benzidine and another aromatic compound (i.e., anthraquinone-based dyes are difficult to degrade due to their fused aromatic ring structure). Certain dispersed dyes are bioaccumulative, and in sediments, the azo and nitro compounds are reduced, transforming other dye-

accumulating substrates into toxic amines. (e.g., R_1-N=N-R_2 + $4H^+$ + $4e^-$ ⟶ R_1-NH_2 + R_2-NH_2).

Because of their carcinogenic nature, the discharge of synthetic and chemically active dyes into industrial effluent is a major environmental problem. Furthermore, the presence of these dyes can obstruct sunlight and reduce oxygen solubility, resulting in reduced photosynthetic activity in aquatic biota [129,146,147].

As a result, it is critical to cleanse these colorful effluents before they enter aquatic bodies. For example, in the standard Salmonella mutagenicity assay, a large group of aromatic amines can either be suspect cancer agents or establish mutagensIn the case of azo dyes, the enzyme-mediated production of genotoxic aromatic amines as metabolites is feasible, which could lead to the creation of the bladder carcinogen benzidine in the human body. [148,149]. The amaranth dyes have been identified as carcinogenic and have been removed from the market [136].

Furthermore, because of the increasingly tight regulations on the organic composition of industrial effluents or pollutants, eliminating dyes from wastewater before they can be released into the environment is critical. However, due to their synthetic origin and very complicated structure, many dyes are difficult to decolorize or disintegrate. These dyes often come in various structural forms, such as acidic, basic, azo, diazo, disperse, anthraquinone-based, naphtha-based, and metal complex dyes [150].

For the treatment of colored wastewater, various physicochemical techniques, such as dye removal or decolorization, have been used. These processes include precipitation, flocculation, electro-kinetic coagulation, electro-flotation, ion exchange, membrane filtration, electrochemical destruction, irradiation, and ozonation. However, all of these treatment systems are expensive, have significant limitations, and cannot be used by small businesses to treat a wide spectrum of wastes [151].

As a result of the chemical stability of these contaminants, typical wastewater treatment systems are significantly inadequate in dealing with synthetic dye-contained wastewater [152]. To lessen the environmental impact of synthetic dyes in wastewater, various treatments have been developed. As a result, precipitation by chemical species, adsorption on the organic or inorganic adsorbent, and degradation by photo-catalysis and/or chemical oxidation processes are some of the technologies now used for synthetic dye removal [150].

3. TiO_2 Based Photo-catalyst

3.1. Structure.

The diameters of titanium dioxide nanoparticles are less than 100 nm [153].

TiO_2 can be found in a variety of rocks and mineral sands. TiO_2 is naturally reddish-brown to black. The color is caused by iron, chromium, vanadium, and zirconium contamination, which can account for up to 10% of the total titanium content [154]. Titanium is the earth's ninth most abundant element. TiO_2 is an odorless, white powder with a molecular weight of 79.9 g/mol, a melting point of 1843 C^0, a boiling point of 2972 C^0, and a relative density of 4.26 g/cm3 at 25 C^0. TiO_2 is insoluble in water, dilute acids, and organic solvents but soluble at high temperatures in concentrated sulfuric or hydrofluoric acids [155].

TiO_2 crystallographic structures are rutile, anatase, and brookite mentioned in Figure 1 [156]. Only rutile and anatase surfaces, which have a crystalline structure and photocatalytic activity, have been studied. TiO_2 anatase and rutile structures are formed by encircling each

Ti^{4+} ion with an octahedron of six O_2 ions, with the oxygen ions surrounded by three other Ti^{4+} ions [157–160]. Ti-Ti distance is longer in anatase, and the Ti-O distance is shorter than in rutile. Each octahedron in the rutile structure is in contact with ten other octahedrons. Each octahedron in the anatase structure has eight neighbors. Because of these differences, the electronic band structures of anatase and rutile differ [157].

At very low temperatures, brookite transforms into rutile. Rutile is the most stable phase in terms of thermodynamics [161,162]. When the temperature exceeds 700° C, the anatase phase irreversibly transforms into a rutile [156,163]. Conversely, the anatase phase will be more stable when the particle size is less than 11 nm. Rutile is stable in aqueous media under very acidic conditions, whereas anatase can be transformed under basic conditions [163].

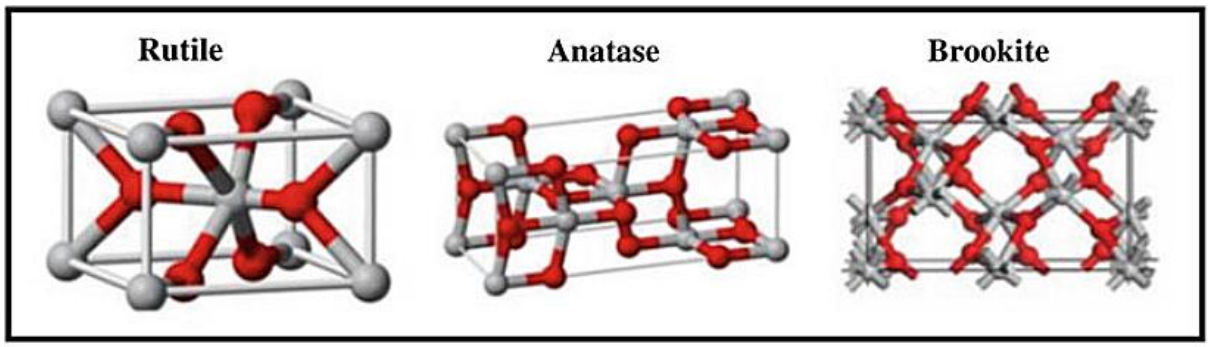

Figure 1. Crystal structures of TiO_2 [164].

3.2. Electrical properties.

Anatase has a band gap energy of E = 3.2 eV for rutile and E = 3.02 eV for brookite, and the wavelength required for activation is less than 387 nm [165,166]. La valeur de bande interdite peut être influencée par La taille des particules [167]. TiO_2 absorbs UV radiation, the energy of which is higher than the energy of the forbidden band. The photons excite the electrons of the valence band (BV) towards the conduction band (BC), creating electron/hole pairs (e/h+) [168]. Independently of the crystalline phase, the BVs, and BCs in TiO_2 are formed from the hybridization of the O2p and Ti3d levels [169].

The particle size can affect the bandgap value [167]. TiO_2 absorbs UV radiation with an energy greater than that of the gap band; the photons excite electrons from the valence band (VB) to the conduction band (CB), resulting in electron/hole pairs (e- / h +) [168]. VBs and CBs in TiO_2 are formed by hybridizing O2p and Ti3d levels, regardless of the crystalline phase [169].

3.3. Synthesis of TiO_2 nanoparticles.

Figure 2 shows method most commonly used methods for producing TiO_2 nanoparticles: sol-gel method, hydrothermal and solvothermal methods, chemical vapor deposition (CVD), micro-emulsion method, electrodeposition, anodic oxidation, sonochemical method, and microwave method [170].

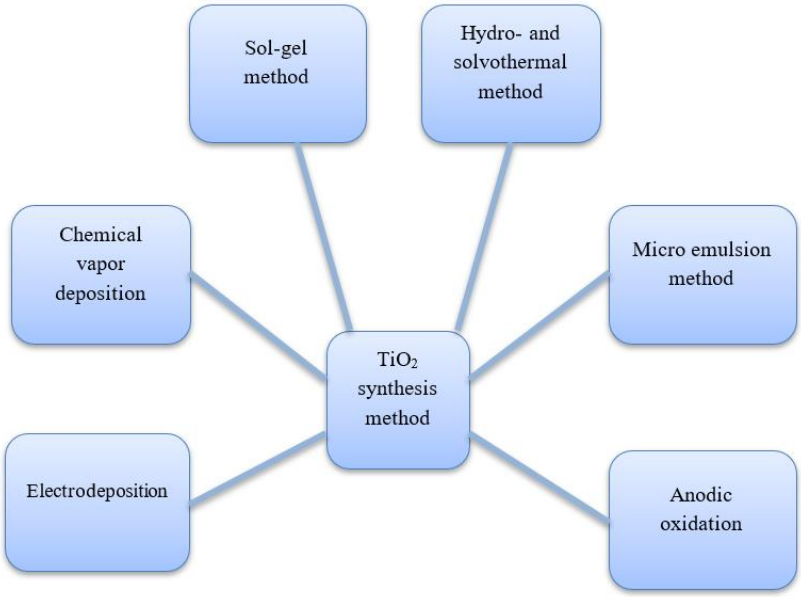

Figure 2. The methods used in the synthesis of TiO_2 nanoparticles.

3.3.1. Sol-gel.

The sol-gel method is the most commonly used because it has several advantages, including high homogeneity, purity, low cost, low-temperature processing, and the ability to control the morphology [171,172].

Titanium (IV) alkoxide is commonly used in the sol-gel method due to its high activity in reactions due to its high electronegative (-OR group), and its reactivity increases with the presence of moisture, heat, and light. The sol-gel process necessitates using a suitable solvent (alkoxide and water do not mix), and alcohols are commonly used as solvents. As catalysts, this process employs acids (acetic acid, hydrochloric acid, hydrofluoric acid) or bases (ammonium hydroxide) [171].

The disadvantages of this method are that the precursor is expensive and sensitive to moisture, the process is done in stages and takes a long time, and the template material is limited [173].

The sol-gel method is based on the gelation of an organometallic precursor solution and the gradual formation of a three-dimensional network through hydrolysis-condensation reactions [172,174].

3.3.2. Chemical vapor deposition (CVD).

The chemical vapor deposition method involves depositing vapors from chemical reactions on a heated surface while maintaining a vacuum. The most important advantage of the chemical vapor deposition method is the homogeneous coating of all sides of the coated material, commonly used in industry to produce thin films [170,175].

Surface morphology is closely related to substrate temperature. A thinner particle-size coating is formed at lower substrate temperatures, whereas a larger particle-size coating is formed at higher substrate temperatures [176]. The main drawbacks of this method are the high process temperature (1000 C^0), geometric distortions, and dimensional changes in the resulting products [177].

In an oxygen-containing atmosphere, titanium tetraisopropoxide is a precursor in preparing thick and fine particle sizes [178]. Recently, modified CVD techniques such as

plasma-enhanced chemical vapor deposition (PECVD), metal-organic chemical vapor deposition (MOCVD), and low-pressure chemical vapor deposition (LPCVD) have been used to create TiO_2 nanoparticles [179–181].

3.3.3. Hydro- and solvothermal methods.

This method is used to synthesize many metal oxide nanoparticles, and it involves dissolving TiO_2 precursors in an aqueous (hydrothermal) or an organic (solvothermal) solution at temperatures ranging from 100°C to 350°C and under high pressure in a sealed Teflon autoclave. Temperature or the addition of salts (NaCl, $SnCl_4$, NH_4Cl) [171] can control the size, whereas hydrolysis and condensing conditions can control morphology [176,182–185].

The hydrothermal method has numerous advantages, including controllable crystal size, morphology, degree of agglomeration, low temperatures sufficient for production, and a high reaction rate [177]. The hydrothermal method is used in water temperatures above 100 C^0 and pressures above 1 bar. The main disadvantage of the hydrothermal method is the requirement for an expensive autoclave system [186].

By using organic solvents with high boiling points, the solvothermal method can work at higher temperatures than the hydrothermal method. Furthermore, the solvothermal method has better control over crystallinity, TiO_2 size, and shape distribution than the hydrothermal method [176].

3.3.4. Micro-emulsion method.

Micro-emulsions are thermodynamically stable solutions composed of a hydrophilic (usual water) phase, a hydrophobic (usual oil) phase, and a surfactant. Reverse micelles are formed when the molar ratio of surfactant/water is less than 15. When it is very high, it is referred to as a micro-emulsion system. The main advantage of the micro-emulsion method is that high temperatures and pressure are not required. Process parameters can easily control the shape, size, and crystal structure of particles. In other words, the particle could be synthesized in the desired morphology [187].

3.3.5. Electrodeposition.

Electrochemical deposition is a technique for depositing inorganic materials on solid surfaces. This method involves oxidizing the metal in its basic form and reducing the metal ions in the solution at the cathode. Coating speeds are very slow with this method, and thicknesses can be controlled. The low synthesis cost and the fact that the process is carried out at a low temperature and atmospheric pressure are two advantages of this method [171]. There are also studies on the deposition of TiO_2 particles using various solutions and electrodes [188,189].

3.3.6. Anodic oxidation.

Anodic oxidation is based on forming an oxide film on the anode's surface because of metal and oxygen ion diffusion and applying an electric field. This method has several advantages, including high reproducibility, ease of application, and low cost [190]. This method can use two types of electrolytes: acidic and alkali electrolytes. Acidic electrolytes can form an oxide and have a wider range of applications than basic electrolytes [191]. The surface

morphology, thickness, and phase structure of the TiO_2 film are directly affected by parameters such as electrolyte type and density, applied voltage, and anodizing time.

The potentials must be low (1 to 130 V) to form a smooth, amorphous, and thin oxide layer (3 to 100 nm), whereas the thick layer and porous morphology are formed at high potentials (100 - 250 V) [192]. The anodic oxidation method results in good nanoparticle adhesion to the surface, which is why TiO_2 nanoparticles obtained by this method are used in the aeronautics and aerospace industries [193].

4. Application Areas

Titanium dioxide has a wide range of applications in the industry due to its excellent optical, electrical, and antibacterial properties and chemical stability. Paint (51 percent of total production), plastic (19 percent), and paper are the most used industries (17 percent). It's also used in the cosmetic and pharmaceutical industries [194].

With the discovery of TiO_2's photocatalytic activity, the material's applications have expanded. TiO_2 nanoparticles are well-known photo-catalysts used in environmental applications and water depollution. The interaction of TiO_2 and ultraviolet light mineralize organic pollutants in CO_2 and H_2O, preventing bacterial growth. TiO_2 nanoparticles can also be used to make anti-fogging and self-cleaning glasses.

However, one of TiO_2's limiting properties is its low activity as a photo-catalyst in visible light. Many studies have shown that processes like doping with metal or nonmetal, as well as co-doping with metal and nonmetal, can increase the photocatalytic activity of TiO_2 in visible light [195]. When TiO_2 nanoparticles absorb light with an energy greater than their bandgap, the hydroxyl group, water, and oxygen at the TiO_2 surface undergo oxidation and reduction reactions, forming reactive oxygen species such as OH, HO_2, and H_2O_2. These organisms break down the organic pollutant. As a result, bacteria, viruses, and tumor cells are killed.

Anatase-structured TiO_2 is used in dye-sensitized solar cells (DSSCs) because it is less expensive, more abundant, and performs better than other semiconductor oxides. To achieve high solar cell efficiency, the semiconductor's bandgap must be large, which TiO_2 (3.2 eV) has. TiO_2 is a semiconductor with a relatively large bandgap (3.2 eV) [196].

The detection of gases by TiO_2 nanoparticles is based on gas molecules modifying the electronic conductivity of TiO_2 film. The chemical stability and porosity of the sensing agent's surface area are critical parameters in gas sensors. TiO_2 gas sensors outperform other metal oxides in terms of stability and sensitivity during high-temperature operations [197].

Titanium dioxide is widely used as a pigment in various industries (paint, plastic, textile, and so on). TiO_2 is opaque, does not produce a lot of dust, and has good paint dispersion. TiO_2 has varying opacity properties. Rutile has more opacifying properties than anatase (refractive index 2.72). (Refractive index 2.52) [198].

TiO_2 is only used in sunscreens because it can absorb UV-A (320–400 nm) and UV-B (290–320 nm) rays [199].

Because TiO_2 nanoparticles are cytocompatible and more sensitive to cells than X-ray beams, they are used in radiotherapy. As a result, it can be used as a radiologic contrast agent [200].

TiO_2 nanoparticles are also used in various applications, as represented in Figure 3, including photocatalytic hydrogen production, energy storage, water purification, self-cleaning fabrics, and optical and electronic storage.

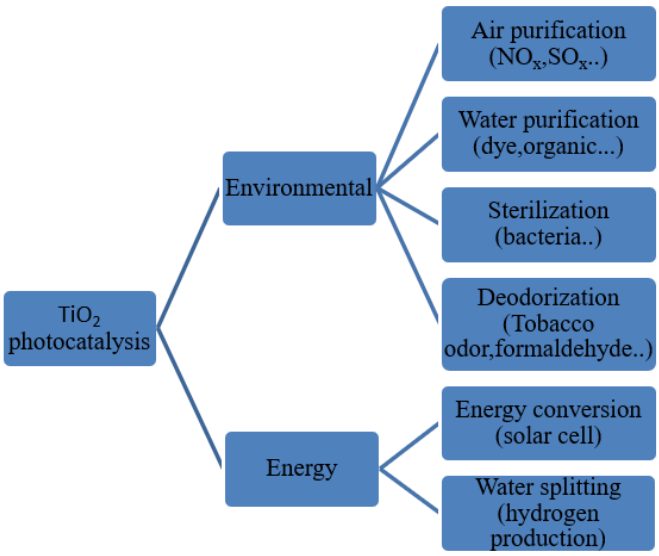

Figure 3. Applications fields of TiO_2 NPs.

4.1. Photo-catalysis.

Heterogeneous photo-catalysis is an advanced oxidation process allowing to catalyze a chemical reaction on the surface of the semiconductor thanks to species such as (HO° radical, $O_2^{\cdot-}$ superoxide radical) produced by reactions of oxidation and reduction of species (H_2O, HO^-, O_2) present on the surface of the catalyst [201]. It has the advantage of allowing the degradation of organic pollutants at room temperature and atmospheric pressure.

The heterogeneous photo-catalysis process consists of five independent steps represented in Figure 4 [202,203]:

1) Transfer of reagents from the liquid phase to the surface of the photo-catalyst
2) Adsorption of reagents at the surface of the photo-catalyst
3) Photocatalytic reaction in the adsorbed phase
4) Desorption of intermediate or final products
5) Transfer of these products within the fluid

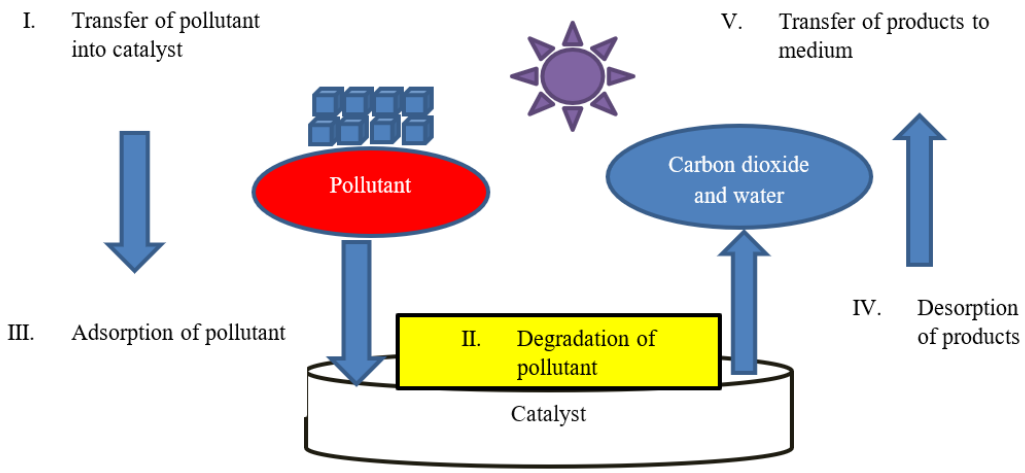

Figure 4. A schematic of photocatalytic reaction steps.

The most used elements in photo-catalysis are semiconductors such as TiO_2, ZnO, SnO_2, ZnS, WO_3, and CdS [204–209]. According to the bandgap of the semiconductor used, we can find the absorption wavelength of the different materials, which is defined by the Planck relationship:

$$\lambda = hc / \Delta E$$

With, h: Planck constant (h = 6.6256 10-34 J.S), C: speed of light (C = $3.0*10^{-8}$ $m.S^{-1}$), E: excitation energy (eV).

The mechanism of photocatalytic degradation of pollutants has been shown in Figure 5.

Equation I.1 gives the excitation of TiO_2 particles under UV irradiation [202,210].

$$TiO_2 + h\nu \longrightarrow TiO_2 (e^-_{CB} + h^+_{VB}) \quad I.1$$

$$h^+ + e^- \longrightarrow \text{Chaleur} \quad I.2$$

Recombination of charge can occur either in the semiconductor bulk or at the surface resulting in the release of heat (or light) and is decrease the photocatalytic activity as the redox reaction of the semiconductor is quenched [202,211–214].

Equation I.2 shows the e^-/h^+ recombination and the energy loss in the form of crystal warming 19.

Photoelectrons react with adsorbed oxygen (O_2) on the semiconductor surface according to reaction (1) and, subsequently, reactions (2) and (3), ultimately resulting in the formation of radicals free (HO°) [215].

$$O_{2,ads} + e^-_{CB} \longrightarrow O^{\circ -}_{2,ads} \quad (1)$$

$$O^{\circ -}_{2,ads} + H^+_{ads} \longrightarrow HO^{\circ}_{2,ads} \quad (2)$$

$$HO^{\circ}_{2,ads} + e^-_{CB} + H^+_{ads} + H_2O_{2,ads} \xrightarrow{h\nu, Ti^{3+}, O_2^{-\circ}} 2\ HO^{\circ}_{ads} \quad (3)$$

In addition, the holes react with water and hydroxyl ions adsorbed on the semiconductor surface, according to reaction (4):

$$H_2O_{ads} + h^+_{VB} \rightarrow HO^{\circ}_{ads} + H^+_{ads}$$

$$HO^-_{ads} + h^+_{VB} \rightarrow HO^{\circ}_{ads} \quad (5)$$

The hydroxyl radicals formed in reactions (3) and (4), and (5) are endowed with an oxidizing power and, therefore, also participate in the degradation of pollutants according to reaction (6):

$$HO^{\circ}_{ads} + PO_{ads} \Longrightarrow CO_2 + H_2O \text{ [216]}$$

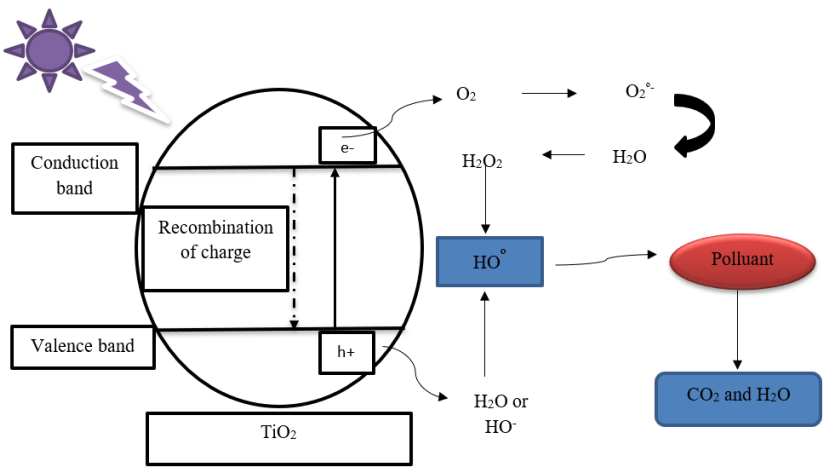

Figure 5. Illustration of photocatalytic degradation mechanism.

The photo-catalysis performances are affected by several parameters such as mass/concentration, light intensity [217], wavelength, pH [218], temperature [219], the nature of a photo-catalyst, Particle Size, Surface area, the adsorption nature, and concentration of the substrate [220,221].

5. TiO_2 photo-catalysis supported in PMMA

Photo-catalysts are generally difficult to recycle; because of the high-cost requirements, separating TiO_2 catalyst from the solution after treatment may pose a barrier to their use in the disposal of industrial wastewater [45,54,70,222].

Since then, unaccompanied metal oxide nanoparticles dispersed liberally in water media have suffered from poor recovery and reusability, potentially limiting their catalytic efficiency [223]. At the same time, the TiO_2 that is supported is easily collected for re-use. Furthermore, it maintains a high specific surface area, producing good photocatalytic activity.

However, there are substantial constraints to the usage of nanomaterials in terms of the consequences on human health and ecosystems due to their use [70,71].

TiO_2 photo-catalyst particles aggregate easily and lose activity [68,69]. Recently, it was claimed that nanostructured TiO_2 fixation on appropriate carriers could be a viable solution to the problem [84–86].

Recent research activities have concentrated on using nanomaterials such as nano-TiO_2 in polymer composites to remove water pollutants [224].

Many techniques for immobilizing TiO_2 on solid supports, such as glass, glass beads, quartz, silica, activated carbon, fiberglass cloth, zeolites, stainless steel, ceramics, clothes, monolith, and polymer membranes, have been proposed [93].

TiO_2 immobilization on a polymer, particularly a transparent support, has also been reported [95,96,222].

The immobilization of TiO_2 nanoparticles in a polymer matrix eliminates the need for a separation process after water purification and, to some extent, avoids the problems associated with ecotoxicity [83].

Polymers are typically low-cost, lightweight, flexible, chemical resistant, mechanically stable, high durability, and easily processed substrates, making them ideal for immobilizing semiconductors for heterogeneous photocatalytic applications [73,75,76,97].

TiO_2 photocatalytic efficiency could be increased by coupling/doping or deposition on support materials such as chitosan, graphene, and methyl methacrylates [225,226].

5.1. PMMA.

Poly(methyl methacrylate) (PMMA) is an optically clear (transparent) thermoplastic that is widely used as a replacement for inorganic glass due to its lightweight with a density of 1.17–1.20 g/cm^3, high impact strength, shatter-resistance, and favorable processing conditions [97,108,109].

The PMMA film is a low-cost, non-spongy solid stable at high temperatures and pH [201,227]. PMMA swells and dissolves in a wide range of organic solvents, but it has poor chemical resistance due to the ester groups that are easily hydrolyzed [228]. It is widely used in physics in optical fibers, optical sensors, LEDs, and other applications [104,201]. Other applications for PMMA include biomedical applications [97] and photocatalysis [105].

PMMA improved UV-light absorption and visible light transparency, as well as the material's storage modulus [229].

Although poly (methyl methacrylate) (PMMA) has high mechanical stability, its use is limited due to the high surface energy of nano-TiO_2 that causes particle aggregation. The question of achieving high nanoparticle dispersion in the organic polymer matrix has become a hot research topic [56,57].

Poly (methyl methacrylate) (PMMA) is a great support for reactive inorganic particles; in particular, the incorporation of TiO_2 into a PMMA matrix has attracted a lot of attention because of the enhancement in the glass transition temperature and thermal properties of the composites [74,110,112,230].

However, there has been little focus on the applications of PMMA–TiO_2 nanocomposites for water purification.

PMMA provided materials with stability and surface area, allowing pollutants to adsorb on the materials easily and •OH to degrade easily.

Polymers in nanofiber form have an extremely high specific surface area [117,118,231]. Resulting in quantum efficiency, a nanoscale effect with unusually high surface energy, surface reactivity, high thermal and electrical conductivity, and biodegradability. Polymer nanofibers are very interesting for various applications, including catalyst supports, drug delivery systems, photonics, and sensors [119].

5.1.1. Synthesis of the nanocomposite.

5.1.1.1. Electrospinning.

Electrospinning is a one-of-a-kind process for producing nanofibers using an electrically charged jet of polymer solution [121,232]. The electrospinning process can produce pure polymer nanofibers and composite [50,124] and blend [125,126] nanofibers. Electrospinning of polymer matrix with functional fillers can improve the electrical properties [124], surface hydrophobicity [126], and thermal properties [125,126] of pure nanofiber. Electrospinning (ES) is a recently developed method for producing nanostructured inorganic semiconductors such as TiO_2 [201].

A particular amount of polymer was dissolved in the solvent, and then semiconductor nanoparticles and surfactants were added to the solution.

After dispersing the solution with ultrasonic for 30 minutes at 50 C^0, the spinning solution was placed into a plastic syringe. A high-voltage supply was connected to the pinhead [233]. The collector aluminum foil was placed at a specific distance from the pinhead's tip [234].

5.1.1.2. Film by sonication and casting method.

By dissolving the polymer in the solvent, a cast solution was formed. The mixture was spun for 24 hours at 25 C^0, then left to stand for another 24 hours. The polymer solution is then distributed on a glass plate with a squeegee. It should be mentioned that the glass plate was dusted with a tiny layer of semiconductor before spreading the polymer, which permits the solid particles to be mechanically fixed on the polymer. The produced film can cure for 60 minutes to allow the solvent to drain before being washed multiple times with distilled water at 25 C^0 to remove any semiconductor particles that did not adhere to the polymer [1].

5.1.1.3. Suspension polymerization.

To begin, the organic phase, which included a photo-initiator and monomer and organic solvents, was vigorously mixed with the semiconductor to ensure homogenous dispersion.

Polyvinyl alcohol (PVA) and 500mL deionized water were used for the water phase. Second, the organic and water phases were combined in the reactor with three vertical baffles and kept oxygen-free by continually purging with nitrogen gas. Finally, the reactive temperature rose to 50°C in 1 hour, stayed at 60°C for 2 hours, and reached 80°C in 1 hour [235].

6. Photocatalytic Activities

Table 2 shows the photocatalytic activity of some TiO_2-PMMA nanocomposites and their recyclability, and their method of synthesis.

The TiO_2-PMMA exhibits high photocatalytic activity in UV light (more than 90%) but moderate in visible light and sunlight (between 30-70%); the nanocomposite can be recovered by sample precipitation of polymer fiber and the use of film.

The use of TiO_2 in the anatase phase or with a high ratio of the anatase phase gives high photocatalytic activity compared with the rutile phase.

Table 2. Summary of photocatalytic activity of some TiO_2-PMMA nanocomposites.

Photocatalysts	**Crystal Phases of TiO_2**	**Method of synthesis of PMMA**	**catalyst**	**Light Source and**	**Target Pollutant**	**Degradation Rate**	**Cycle**	**Ref.**
γ-Fe_2O_3/PMMA/S-TiO_2 core/shell	anatase	Modified suspension polymerization	1g/l	Philips 25WFluorescent	Phenanthrene 2mg/l	96.5%	5 86.5%	[235]
Fiber TiO_2-PMMA	-	Electrospinning and RF Magnetron Sputtering of TiO2 Layers	-	solar simulator's white light	Rhodamine B	95% for the TiO2 nanotubes and 55% for the ZnO nanotubes after 600min	-	[50]
TiO_2-PMMA	P25	Film	15mg of blend TiO_2-PMMA	solar lamp Wattage 300 W, Radiated Power: (315–400 nm) 13.6 W, (280–315 nm) 3.0 W, Wavelength range 280–1000 nm	Methylene Blue, Rhodamine B, Paraquat and Acetaminophen	65% for methylene blue and 35% for Rhodamine B after 120min 51% for parquet and 40% for paracetamol after 480min	-	[37]
TiO_2-P(MMA-co-BA-co-MTC) membranes	TiO_2-P25	*In situ* photopolymerization	2g of a membrane with 0.5% TiO_2	LED light (365 nm, 7 W)	methylene blue 6ppm	100% after 270min	-	[32]
Xylan-g-PMMA/TiO2 Nanofibers	TiO_2 NPs	Electrospinning	mats of 6 × 2.5 cm^2 with 10 or 30% TiO_2	125 W ultraviolet light (365–400 nm)	methylene blue 20ppm	80% after 300min	-	[232]:
TiO_2@PMMA	anatase	Electrospinning	1g	32 W high-pressure	methyl orange MO 10mg/l	94.4% after 50min	5 94.4%	[234]

Photocatalysts	Crystal Phases of TiO_2	Method of synthesis of PMMA	catalyst	Light Source and	Target Pollutant	Degradation Rate	Cycle	Ref.
		combined with hydrothermal synthesis		mercury lamp				
TiO_2-PMMA	anatase	Electrospinning	10 mm × 10 mm with 5 or 10% TiO_2	UV lamp 400F/2, UVASPOT 400/T	methylene blue (2 × 10−5 mol/L)	95.8% for 5% TiO_2 and 99.1 % for 10% TiO_2 after 3h	3 cycles maintain their photocatalytic activity	[201]
nano-TiO_2/poly(methylmethacrylate) nanofibres	anatase	Electrospinning	10% TiO_2	Sunlight	methyl orange	Up to 50% after 5h	-	[233]
PMMA / TiO_2 nanofibers	Anatase and rutile	electrospinning	10% TiO_2	sunlight	methyl orange solution 10 mg/L	51.3% for anatase 28.8% for rutile After 5h	-	[236]
PMMA/TNTs		method of sonication and solution casting	15% TNTs	UV light (TL 8W BLB 1FM, Philips)	2ml of aqueous solution of MB(0.355mg/L)	100% after 240min	5 100%	[237]
N/TiO_2_P25	A/R=3.5	*wet impregnation method*	30mg	UV light source, TUV 16W 4P SE UNP/32	200 mL of 20 mg/L methylene blue	99.9% after 180min	-	[238]
			60 mg	a visible light source, MASTER TL-D Eco 16W/840 1SL	400 mL of 20 mg/L methylene blue	70% after 180min		
TiO_2_P25-g-PMMA	A/R=3.7	ATRP technique	PMMA film, 5x10 cm and 10x 20 cm	under UV light(16W)	200 mL of 20 mg/L methylene blue	95.5% after 180min	-	[238]
				visible light(16W)	500 mL of 20 mg/L methylene blue	33.6% after 180min		
N/TiO_2_P25-g-PMMA	A/R=3.5	ATRP technique	PMMA film, 5x10 cm and 10x 20 cm	UV light(16W)	200 mL of 20 mg/L methylene blue	99.2% after 180min	-	[238]
				visible light(16W)	500 mL of 20 mg/L methylene blue	63.2% after 180min		
Si/TiO_2_FSP	A/R=5.1	*flame spray pyrolysis method*	30mg	UV light source, TUV 16W 4P SE UNP/32	200 mL of 20 mg/L methylene blue	99.9% after 180min	-	[238]
			60 mg	a visible light source, MASTER TL-D Eco 16W/840 1SL	400 mL of 20 mg/L methylene blue	57.2% after 180min		
Si/TiO_2_FSP-g-PMMA	A/R=5.1	ATRP technique	PMMA film, 5x10 cm and 10x 20 cm	under UV light(16W)	200 mL of 20 mg/L methylene blue	97% after 180min	-	[238]
				visible light(16W)	500 mL of 20 mg/L methylene blue	59.3% after 180min		

Photocatalysts	Crystal Phases of TiO_2	Method of synthesis of PMMA	catalyst	Light Source and	Target Pollutant	Degradation Rate	Cycle	Ref.
PMMA/TiO_2 nanofiber mat	-	electrospinning	samples (8*8 cm2)	UV light (8w)	50 ml methylene blue (10 mg/L)	20% after 180min	-	[239]
TiO_2/PMMA film	anatase	cast solution	5cm/5 cm film	9W UV-A Lamp	200 mL methylene blue (2.5 mg/ L)	30% after 200min	-	[1]
TiO_2/CNTs/PMMA	anatase	electrospinning		high-pressure mercury lamp(32w)	100ml MO (10mg/l)	100% after 50min	10 95%	[231]
MoS_2@TiO_2@PMMA	anatase	electrospinning	100 mg	32W high-pressure mercury UV lamp	100ml MO (10mg/l)	95.7% after 50min	10 95.6%	[240]

7. Conclusion

Due to its peculiar electronic structure, which includes a filled valence band and an empty conduction band, TiO_2 works as a photo-catalyst for light-induced photochemical reactions. The redox potential for the evolution of hydrogen and oxygen from water and the creation of reactive oxygenated species must be within the semiconductor bandgap for an efficient TiO_2 photo-catalyst. Indeed, the TiO_2 photo-catalyst must be highly stable in various pollutant concentrations and kinds. Photocatalytic treatment is an effective method for treating dye chemicals in wastewater effluent.

Persistent efforts are being made to modify the TiO_2 photo-catalyst to make it more effective in visible light while facilitating post-treatment recovery. We attempted to outline the key properties of PMMA-supported TiO_2 photo-catalysts and their efficacy in degrading refractory pollutants, particularly dyes, from wastewater in this review paper. As a result, we conclude that while PMMA-supported titanium dioxide photo-catalysts have been effectively created for wastewater cleanup in the laboratory, much work remains to be done before they can be commercialized. The potential nature of PMMA-supported TiO_2 photo-catalysts necessitates more research into developing successful, low-cost, bandgap re-engineering, widely dispersed, highly adsorbed, and reusable photo-catalysts, as well as simple procedures for their fabrication. The emphasis should be on producing PMMA-supported TiO_2 photo-catalysts that are not only extremely effective in visible and/or solar light but can also be reused for several runs with no appreciable decrease in photocatalytic activity. Combining support materials with TiO_2 in large-scale production is anticipated to be beneficial for industrial dye wastewater treatment.

Funding

This research received no external funding.

Acknowledgments

This research has no acknowledgment.

Conflicts of Interest

The authors declare no conflict of interest.

References

1. Ounas, O.; El Foulani, A.A.; Lekhlif, B.; Jamal-Eddine, J. Immobilization of TiO2 into a Poly Methyl Methacrylate (PMMA) as Hybrid Film for Photocatalytic Degradation of Methylene Blue. *Mater. Today Proc.* **2020**, *22*, 35–40, https://doi.org/10.1016/j.matpr.2019.08.068.
2. Global Water Pollution and Human Health | Annual Review of Environment and Resources Available online: https://www.annualreviews.org/doi/full/10.1146/annurev-environ-100809-125342 (accessed on 8 January 2022).
3. Chan, S.H.S.; Yeong Wu, T.; Juan, J.C.; Teh, C.Y. Recent Developments of Metal Oxide Semiconductors as Photocatalysts in Advanced Oxidation Processes (AOPs) for Treatment of Dye Waste-Water. *J. Chem. Technol. Biotechnol.* **2011**, *86*, 1130–1158, https://doi.org/10.1002/jctb.2636.
4. Raizada, P.; Singh, P.; Kumar, A.; Pare, B.; Jonnalagadda, S.B. Zero Valent Iron-Brick Grain Nanocomposite for Enhanced Solar-Fenton Removal of Malachite Green. *Sep. Purif. Technol.* **2014**, *133*, 429–437, https://doi.org/10.1016/j.seppur.2014.07.012.
5. Bouziane Errahmani, K.; Mahmoudi, H.; Goosen, M.; Benhabiles, O.; Bengharez, Z.; Bellebia, S. Photocatalytic Nanocomposite Polymer-TiO2 Membranes for Pollutant Removal from Wastewater. *Catalysts* **2021**, *11*, https://doi.org/10.3390/catal11030402.
6. Yang, H.; Cheng, H. Controlling Nitrite Level in Drinking Water by Chlorination and Chloramination. *Sep. Purif. Technol.* **2007**, *56*, 392–396, https://doi.org/10.1016/j.seppur.2007.05.036.
7. Miller, J. Review of Water Resources and Desalination Technologies. *Water Treatment* **2003**, https://doi.org/10.2172/809106.
8. Alkayal, N.S.; Altowairki, H.; Alosaimi, A.M.; Hussein, M.A. Network Template-Based Cross-Linked Poly(Methyl Methacrylate)/Tin(IV) Oxide Nanocomposites for the Photocatalytic Degradation of MB under UV Irradiation. *J. Mater. Res. Technol.* **2022**, *18*, 2721–2734, https://doi.org/10.1016/j.jmrt.2022.03.133.
9. Wu, Y.; Lu, L.; Zhang, Y.; Yuan, Z.; Yang, L.; Wang, L.; Rao, Y. A Bioinspired Cercosporin/Polymethylmethacrylate Photocatalyst with High Efficiency for Decontamination of Pharmaceuticals and Pathogens. *J. Hazard. Mater.* **2021**, *419*, https://doi.org/10.1016/j.jhazmat.2021.126555.
10. Sudhaik, A.; Raizada, P.; Shandilya, P.; Singh, P. Magnetically Recoverable Graphitic Carbon Nitride and NiFe2O4 Based Magnetic Photocatalyst for Degradation of Oxytetracycline Antibiotic in Simulated Wastewater under Solar Light. *J. Environ. Chem. Eng.* **2018**, *6*, 3874–3883, https://doi.org/10.1016/j.jece.2018.05.039.
11. Micheal, K.; Ayeshamariam, A.; Boddula, R.; Arunachalam, P.; AlSalhi, M.S.; Theerthagiri, J.; Prasad, S.; Madhavan, J.; Al-Mayouf, A.M. Assembled Composite of Hematite Iron Oxide on Sponge-like BiOCl with Enhanced Photocatalytic Activity. *Mater. Sci. Energy Technol.* **2019**, *2*, 104–111, https://doi.org/10.1016/j.mset.2018.11.004.
12. Raizada, P.; Sudhaik, A.; Singh, P.; Shandilya, P.; Thakur, P.; Jung, H. Visible Light Assisted Photodegradation of 2,4-Dinitrophenol Using Ag2CO3 Loaded Phosphorus and Sulphur Co-Doped Graphitic Carbon Nitride Nanosheets in Simulated Wastewater. *Arab. J. Chem.* **2020**, *13*, 3196–3209, https://doi.org/10.1016/j.arabjc.2018.10.004.
13. Raizada, P.; Sudhaik, A.; Singh, P.; Shandilya, P.; Saini, A.K.; Gupta, V.K.; Lim, J.-H.; Jung, H.; Hosseini-Bandegharaei, A. Fabrication of Ag3VO4 Decorated Phosphorus and Sulphur Co-Doped Graphitic Carbon Nitride as a High-Dispersed Photocatalyst for Phenol Mineralization and E. Coli Disinfection. *Sep. Purif. Technol.* **2019**, *212*, 887–900, https://doi.org/10.1016/j.seppur.2018.12.007.
14. Chong, M.N.; Jin, B.; Chow, C.W.K.; Saint, C. Recent Developments in Photocatalytic Water Treatment Technology: A Review. *Water Res.* **2010**, *44*, 2997–3027, https://doi.org/10.1016/j.watres.2010.02.039.
15. Gaya, U.I.; Abdullah, A.H. Heterogeneous Photocatalytic Degradation of Organic Contaminants over Titanium Dioxide: A Review of Fundamentals, Progress, and Problems. *J. Photochem. Photobiol. C Photochem. Rev.* **2008**, *9*, 1–12, https://doi.org/10.1016/j.jphotochemrev.2007.12.003.
16. Palmisano, G.; Augugliaro, V.; Pagliaro, M.; Palmisano, L. Photocatalysis: A Promising Route for 21st Century Organic Chemistry. *Chem. Commun.* **2007**, *33*, 3425–3437, https://doi.org/10.1039/B700395C.
17. Pichat, P. *Photocatalysis, and Water Purification: From Fundamentals to Recent Applications*. John Wiley & Sons, **2013**; https://doi.org/10.1002/9783527645404.
18. Cui, B.; Peng, H.; Xia, H.; Guo, X.; Guo, H. Magnetically RecoverableCore–Shell Nanocomposites γ-Fe2O3@SiO2@TiO2–Ag with Enhanced Photocatalytic Activity and Antibacterial Activity. *Sep. Purif. Technol.* **2013**, *103*, 251–257, https://doi.org/10.1016/j.seppur.2012.10.008.
19. Zhou, J.; Chen, M.; Qiao, X.; Wu, L. Facile Preparation Method of SiO2/PS/TiO2 Multilayer Core−Shell Hybrid Microspheres. *Langmuir* **2006**, *22*, 10175-10179, https://doi.org/10.1021/la062220h.

20. Peng, B.; Tang, F.; Chen, D.; Ren, X.; Meng, X.; Ren, J. Preparation of PS/TiO2/UF MultilayerCore–Shell Hybrid Microspheres with High Stability. *J. Colloid Interface Sci.* **2009**, *329*, 62–66, https://doi.org/10.1016/j.jcis.2008.09.069.
21. Zhang, L.; Wang, T.; Liu, P. Superparamagnetic Sandwich Fe3O4@PS@PANi Microspheres and Yolk/Shell Fe3O4@PANi Hollow Microspheres with Fe3O4@PS Nanoparticles as "Partially Sacrificial Templates." *Chem. Eng. J.* **2012**, *187*, 372–379, https://doi.org/10.1016/j.cej.2012.01.125.
22. Murcia-López, S.; Bacariza, M.C.; Villa, K.; Lopes, J.M.; Henriques, C.; Morante, J.R.; Andreu, T. Controlled Photocatalytic Oxidation of Methane to Methanol through Surface Modification of Beta Zeolites. *ACS Catalysis* **2017**, *7*, 2878-2885, https://doi.org/10.1021/acscatal.6b03535.
23. Park, H.; Choi, W. Visible Light and Fe(III)-Mediated Degradation of Acid Orange 7 in the Absence of H2O2. *J. Photochem. Photobiol. Chem.* **2003**, *159*, 241–247, https://doi.org/10.1016/S1010-6030(03)00141-2.
24. Akpan, U.G.; Hameed, B.H. Parameters Affecting the Photocatalytic Degradation of Dyes Using TiO2-Based Photocatalysts: A Review. *J. Hazard. Mater.* **2009**, *170*, 520–529, https://doi.org/10.1016/j.jhazmat.2009.05.039.
25. Noman, M.T.; Ashraf, M.A.; Ali, A. Synthesis and Applications of Nano-TiO2: A Review. *Environ. Sci. Pollut. Res. Int.* **2019**, *26*, 3262–3291, https://doi.org/10.1007/s11356-018-3884-z.
26. Ragheb, N.; Borg, H. Antimicrobial Effect of Titanium Oxide (Tio2) Nano Particles in Completely Edentulous Patients. A Randomized Clinical Trial. *Adv. Dent. J.* **2021**, *3*, 173–184, https://doi.org/10.21608/adjc.2021.91184.1105.
27. Utami, F.D.; Rahman, D.Y.; Sustini, E.; Abdullah, M. Immobilization of TiO2 on Transparent Plastic and Its Application in Photocatalytic Wastewater Treatment. *J. Phys. Conf. Ser.* **2019**, *1171*, https://doi.org/10.1088/1742-6596/1171/1/012030.
28. Priya, B.; Shandilya, P.; Raizada, P.; Thakur, P.; Singh, N.; Singh, P. Photocatalytic Mineralization and Degradation Kinetics of Ampicillin and Oxytetracycline Antibiotics Using Graphene Sand Composite and Chitosan Supported BiOCl. *J. Mol. Catal. Chem.* **2016**, *423*, 400–413, https://doi.org/10.1016/j.molcata.2016.07.043.
29. Sudhaik, A.; Raizada, P.; Shandilya, P.; Jeong, D.-Y.; Lim, J.-H.; Singh, P. Review on Fabrication of Graphitic Carbon Nitride Based Efficient Nanocomposites for Photodegradation of Aqueous Phase Organic Pollutants. *J. Ind. Eng. Chem.* **2018**, *67*, 28–51, https://doi.org/10.1016/j.jiec.2018.07.007.
30. Raizada, P.; Priya, B.; Thakur, P.; Singh, P. Solar Light Induced Photodegradation of Oxytetracycline Using Zr Doped TiO2/CaO Based Nanocomposite. *Indian J Chem* **2016**, *7*.
31. Wang, X.; Li, Q.; Gan, L.; Ji, X.; Chen, F.; Peng, X.; Zhang, R. 3D Macropore Carbon-Vacancy g-C3N4 Constructed Using Polymethylmethacrylate Spheres for Enhanced Photocatalytic H2 Evolution and CO2 Reduction. *J. Energy Chem.* **2021**, *53*, 139–146, https://doi.org/10.1016/j.jechem.2020.05.001.
32. Ma, L.; Chen, Y.; Zheng, J. An Efficient, Stable and Reusable Polymer/TiO2 Photocatalytic Membrane for Aqueous Pollution Treatment. *J. Mater. Sci.* **2021**, *56*, 11335–11351, https://doi.org/10.1007/s10853-021-06018-6.
33. Zheng, X.; Shen, Z.-P.; Shi, L.; Cheng, R.; Yuan, D.-H. Photocatalytic Membrane Reactors (PMRs) in Water Treatment: Configurations and Influencing Factors. *Catalysts* **2017**, *7*, https://doi.org/10.3390/catal7080224.
34. Entradas, T.J.; Cabrita, J.F.; Barrocas, B.; Nunes, M.R.; Silvestre, A.J.; Monteiro, O.C. Synthesis of Titanate Nanofibers Co-Sensitized with ZnS and Bi2S3 Nanocrystallites and Their Application on Pollutants Removal. *Mater. Res. Bull.* **2015**, *72*, 20–28, https://doi.org/10.1016/j.materresbull.2015.07.008.
35. Schaffer, J. Immobilization of TiO2: Via Different Routes for Photocatalytic Reactions in a PDMS Based Microreactor - University of Twente Student Theses Available online: http://essay.utwente.nl/62126/ (accessed on 8 January 2022).
36. Mani, A.D.; Reddy, P.M.K.; Srinivaas, M.; Ghosal, P.; Xanthopoulos, N.; Subrahmanyam, C. Facile Synthesis of Efficient Visible Active C-Doped TiO2 Nanomaterials with High Surface Area for the Simultaneous Removal of Phenol and Cr(VI). *Mater. Res. Bull.* **2015**, *61*, 391–399, https://doi.org/10.1016/j.materresbull.2014.10.051.
37. Nicosia, A.; Vento, F.; Di Mari, G.M.; D'Urso, L.; Mineo, P.G. TiO2-Based Nanocomposites Thin Film Having Boosted Photocatalytic Activity for Xenobiotics Water Pollution Remediation. *Nanomaterials* **2021**, *11*, https://doi.org/10.3390/nano11020400.
38. Karunakaran, C.; Abiramasundari, G.; Gomathisankar, P.; Manikandan, G.; Anandi, V. Preparation and Characterization of ZnO–TiO2 Nanocomposite for Photocatalytic Disinfection of Bacteria and Detoxification of Cyanide under Visible Light. *Mater. Res. Bull.* **2011**, *46*, 1586–1592, https://doi.org/10.1016/j.materresbull.2011.06.019.
39. Fu, J. Photocatalytic Properties of TiO2–P2O5 Glass Ceramics. *Mater. Res. Bull.* **2011**, *46*, 2523–2526, https://doi.org/10.1016/j.materresbull.2011.08.016.
40. Sun, X.; Gong, C.; Lv, G.; Bin, F.; Song, C. Effect of Ce/Zr Molar Ratio on the Performance of Cu–Cex–Zr1−x/TiO2 Catalyst for Selective Catalytic Reduction of NOx with NH3 in Diesel Exhaust. *Mater. Res. Bull.* **2014**, *60*, 341–347, https://doi.org/10.1016/j.materresbull.2014.09.014.

41. Wang, P.; Wang, J.; Yu, H.; Zhao, L.; Yu, J. Hierarchically Macro–Mesoporous TiO2 Film via Self-Assembled Strategy for Enhanced Efficiency of Dye-Sensitized Solar Cells. *Mater. Res. Bull.* **2016**, *74*, 380–386, https://doi.org/10.1016/j.materresbull.2015.11.004.
42. Shengyuan, Y.; Peining, Z.; Nair, A.S.; Ramakrishna, S. Rice Grain-Shaped TiO2 Mesostructures—Synthesis, Characterization, and Applications in Dye-Sensitized Solar Cells and Photocatalysis. *J. Mater. Chem.* **2011**, *21*, 6541–6548, https://doi.org/10.1039/C0JM04512H.
43. Qu, A.; Xu, X.; Xie, H.; Zhang, Y.; Li, Y.; Wang, J. Effects of Calcining Temperature on Photocatalysis of G-C3N4/TiO2 Composites for Hydrogen Evolution from Water. *Mater. Res. Bull.* **2016**, *80*, 167–176, https://doi.org/10.1016/j.materresbull.2016.03.043.
44. Etacheri, V.; Di Valentin, C.; Schneider, J.; Bahnemann, D.; Pillai, S.C. Visible-Light Activation of TiO2 Photocatalysts: Advances in Theory and Experiments. *J. Photochem. Photobiol. C Photochem. Rev.* **2015**, *25*, 1–29, https://doi.org/10.1016/j.jphotochemrev.2015.08.003.
45. Weon, S.; Choi, W. TiO2 Nanotubes with Open Channels as Deactivation-Resistant Photocatalyst for the Degradation of Volatile Organic Compounds. *Environ. Sci. Technol.* **2016**, *50*, 2556–2563, https://doi.org/10.1021/acs.est.5b05418.
46. Gao, L.; Wang, Y.; Yan, Y.; Li, Q.; Hao, C.; Ma, T. Enhanced Photoactivities of TiO2 Particles Induced by Bio-Inspired Micro-Nanoscale Substrate. *J. Colloid Interface Sci.* **2016**, *470*, 10–13, https://doi.org/10.1016/j.jcis.2016.02.029.
47. Arabzadeh, A.; Salimi, A. One Dimensional CdS Nanowire@TiO2 Nanoparticles Core-Shell as High-Performance Photocatalyst for Fast Degradation of Dye Pollutants under Visible and Sunlight Irradiation. *J. Colloid Interface Sci.* **2016**, *479*, 43–54, https://doi.org/10.1016/j.jcis.2016.06.036.
48. Zhang, J.; Li, L.; Xiao, Z.; Liu, D.; Wang, S.; Zhang, J.; Hao, Y.; Zhang, W. Hollow Sphere TiO2–ZrO2 Prepared by Self-Assembly with Polystyrene Colloidal Template for Both Photocatalytic Degradation and H2 Evolution from Water Splitting. *ACS Sustain. Chem. Eng.* **2016**, *4*, 2037–2046, https://doi.org/10.1021/acssuschemeng.5b01359.
49. Basile, A.; Cassano, A.; Rastogi, N.K. *Advances in Membrane Technologies for Water Treatment: Materials, Processes, and Applications*. Elsevier, **2015**; https://doi.org/10.1016/C2013-0-16469-0.
50. Enculescu, M.; Costas, A.; Evanghelidis, A.; Enculescu, I. Fabrication of ZnO and TiO2 Nanotubes via Flexible Electro-Spun Nanofibers for Photocatalytic Applications. *Nanomaterials* **2021**, *11*, https://doi.org/10.3390/nano11051305.
51. Zimbone, M.; Buccheri, M.A.; Cacciato, G.; Sanz, R.; Rappazzo, G.; Boninelli, S.; Reitano, R.; Romano, L.; Privitera, V.; Grimaldi, M.G. Photocatalytical and Antibacterial Activity of TiO2 Nanoparticles Obtained by Laser Ablation in Water. *Appl. Catal. B Environ.* **2015**, *165*, 487–494, https://doi.org/10.1016/j.apcatb.2014.10.031.
52. Scuderi, V.; Impellizzeri, G.; Romano, L.; Scuderi, M.; Brundo, M.V.; Bergum, K.; Zimbone, M.; Sanz, R.; Buccheri, M.A.; Simone, F.; Nicotra, G.; Svensson, B.G.; Grimaldi, M.G.; Privitera, V. An Enhanced Photocatalytic Response of Nanometric TiO2 Wrapping of Au Nanoparticles for Eco-Friendly Water Applications. *Nanoscale* **2014**, *6*, 11189–11195, https://doi.org/10.1039/C4NR02820A.
53. Scuderi, V.; Impellizzeri, G.; Romano, L.; Scuderi, M.; Nicotra, G.; Bergum, K.; Irrera, A.; Svensson, B.G.; Privitera, V. TiO2-Coated Nanostructures for Dye Photo-Degradation in Water. *Nanoscale Res. Lett.* **2014**, *9*, https://doi.org/10.1186/1556-276X-9-458.
54. Sanz, R.; Romano, L.; Zimbone, M.; Buccheri, M.A.; Scuderi, V.; Impellizzeri, G.; Scuderi, M.; Nicotra, G.; Jensen, J.; Privitera, V. UV-Black Rutile TiO2: An Antireflective Photocatalytic Nanostructure. *J. Appl. Phys.* **2015**, *117*, https://doi.org/10.1063/1.4913222.
55. Cacciato, G.; Bayle, M.; Pugliara, A.; Bonafos, C.; Zimbone, M.; Privitera, V.; Grimaldi, M.G.; Carles, R. Enhancing Carrier Generation in TiO2 by a Synergistic Effect between Plasmon Resonance in Ag Nanoparticles and Optical Interference. *Nanoscale* **2015**, *7*, 13468–13476, https://doi.org/10.1039/C5NR02406D.
56. Raja, K.S.; Misra, M.; Paramguru, K. Formation of Self-Ordered Nano-Tubular Structure of Anodic Oxide Layer on Titanium. *Electrochimica Acta* **2005**, *51*, 154–165, https://doi.org/10.1016/j.electacta.2005.04.011.
57. Ou, H.-H.; Lo, S.-L. Review of Titania Nanotubes Synthesized via the Hydrothermal Treatment: Fabrication, Modification, and Application. *Sep. Purif. Technol.* **2007**, *58*, 179–191, https://doi.org/10.1016/j.seppur.2007.07.017.
58. Bavykin, D.V.; Friedrich, J.M.; Walsh, F.C. Protonated Titanates and TiO2 Nanostructured Materials: Synthesis, Properties, and Applications. *Advanced Materials* **2006**, *18*, 2807-2824, https://doi.org/10.1002/adma.200502696.
59. Fujishima, A.; Rao, T.N.; Tryk, D.A. Titanium Dioxide Photocatalysis. *J. Photochem. Photobiol. C Photochem. Rev.* **2000**, *1*, 1–21, https://doi.org/10.1016/S1389-5567(00)00002-2.
60. Diebold, U. The Surface Science of Titanium Dioxide. *Surf. Sci. Rep.* **2003**, *48*, 53–229, https://doi.org/10.1016/S0167-5729(02)00100-0.
61. Fujishima, A.; Zhang, X.; Tryk, D.A. TiO2 Photocatalysis, and Related Surface Phenomena. *Surf. Sci. Rep.* **2008**, *63*, 515–582, https://doi.org/10.1016/j.surfrep.2008.10.001.

62. Daneshvar, N.; Salari, D.; Khataee, A.R. Photocatalytic Degradation of Azo Dye Acid Red 14 in Water: Investigation of the Effect of Operational Parameters. *J. Photochem. Photobiol. Chem.* **2003**, *157*, 111–116, https://doi.org/10.1016/S1010-6030(03)00015-7.
63. Jiang, Y.; Wang, W.-N.; Biswas, P.; Fortner, J.D. Facile Aerosol Synthesis and Characterization of Ternary Crumpled Graphene–TiO2–Magnetite Nanocomposites for Advanced Water Treatment. *ACS Appl. Mater. Interfaces* **2014**, *6*, 11766–11774, https://doi.org/10.1021/am5025275.
64. Schneider, J.; Matsuoka, M.; Takeuchi, M.; Zhang, J.; Horiuchi, Y.; Anpo, M.; Bahnemann, D.W. Understanding TiO2 Photocatalysis: Mechanisms and Materials. *Chem. Rev.* **2014**, *114*, 9919–9986, https://doi.org/10.1021/cr5001892.
65. Altavilla, C.; Ciliberto, E. *Inorganic Nanoparticles: Synthesis, Applications, and Perspectives*. CRC Press, **2017**.
66. Zan, L.; Fa, W.; Wang, S. Novel Photodegradable Low-Density Polyethylene−TiO2 Nanocomposite Film. *Environ. Sci. Technol.* **2006**, *40*, 1681–1685, https://doi.org/10.1021/es051173x.
67. Cho, M.; Chung, H.; Choi, W.; Yoon, J. Linear Correlation between Inactivation of E. Coli and OH Radical Concentration in TiO2 Photocatalytic Disinfection. *Water Res.* **2004**, *38*, 1069–1077, https://doi.org/10.1016/j.watres.2003.10.029.
68. Li, G.; Lv, L.; Fan, H.; Ma, J.; Li, Y.; Wan, Y.; Zhao, X.S. Effect of the Agglomeration of TiO2 Nanoparticles on Their Photocatalytic Performance in the Aqueous Phase. *J. Colloid Interface Sci.* **2010**, *348*, 342–347, https://doi.org/10.1016/j.jcis.2010.04.045.
69. French, R.A.; Jacobson, A.R.; Kim, B.; Isley, S.L.; Penn, R.L.; Baveye, P.C. Influence of Ionic Strength, PH, and Cation Valence on Aggregation Kinetics of Titanium Dioxide Nanoparticles. *Environ. Sci. Technol.* **2009**, *43*, 1354–1359, https://doi.org/10.1021/es802628n.
70. Aruoja, V.; Dubourguier, H.-C.; Kasemets, K.; Kahru, A. Toxicity of Nanoparticles of CuO, ZnO and TiO2 to Microalgae Pseudokirchneriella Subcapitata. *Sci. Total Environ.* **2009**, *407*, 1461–1468, https://doi.org/10.1016/j.scitotenv.2008.10.053.
71. Adams, L.K.; Lyon, D.Y.; Alvarez, P.J.J. Comparative Eco-Toxicity of Nanoscale TiO2, SiO2, and ZnO Water Suspensions. *Water Res.* **2006**, *40*, 3527–3532, https://doi.org/10.1016/j.watres.2006.08.004.
72. School of Fundamental Science, Universiti Malaysia Terengganu, 21030 UMT Kuala Terengganu, Terengganu, Malaysia; Kok Sheng, C. Investigation of Morphological, Structural and Electrical Properties of Cds/ PMMA Nanocomposite Film Prepared by Solution Casting Method. *Int. J. Electrochem. Sci.* **2017**, *12*, 10023–10031, https://doi.org/10.20964/2017.11.75.
73. Jordan, J.; Jacob, K.I.; Tannenbaum, R.; Sharaf, M.A.; Jasiuk, I. Experimental Trends in Polymer Nanocomposites - A Review. *Mater. Sci. Eng. A* **2005**, *393*, 1–11, https://doi.org/10.1016/j.msea.2004.09.044.
74. Hafizah, N.N.; Mamat, M.H.; Said, C.M.S.; Abidin, M.H.; Rusop, M. Thermal Degradation of Nanocomposited PMMA/TiO2 Nanocomposites. *IOP Conf. Ser.: Mater. Sci. Eng.* **2013**, *46*, https://doi.org/10.1088/1757-899X/46/1/012045.
75. Caseri, W. Nanocomposites of Polymers and Metals or Semiconductors: Historical Background and Optical Properties. *Macromol. Rapid Commun.* **2000**, *21*, 705–722, https://doi.org/10.1002/1521-3927(20000701)21:11<705::AID-MARC705>3.0.CO;2-3.
76. Kickelbick, G. *Hybrid Materials: Synthesis, Characterization, and Applications*. John Wiley & Sons, **2007**; https://doi.org/10.1002/9783527610495.
77. Hanemann, T.; Szabó, D.V. Polymer-Nanoparticle Composites: From Synthesis to Modern Applications. *Materials* **2010**, *3*, 3468–3517, https://doi.org/10.3390/ma3063468.
78. Jeon, I.-Y.; Baek, J.-B. Nanocomposites Derived from Polymers and Inorganic Nanoparticles. *Materials* **2010**, *3*, 3654–3674, https://doi.org/10.3390/ma3063654.
79. Paul, D.R.; Robeson, L.M. Polymer Nanotechnology: Nanocomposites. *Polymer* **2008**, *49*, 3187–3204, https://doi.org/10.1016/j.polymer.2008.04.017.
80. Keane, D.A.; McGuigan, K.G.; Ibáñez, P.F.; Polo-López, M.I.; Byrne, J.A.; Dunlop, P.S.M.; O'Shea, K.; Dionysiou, D.D.; Pillai, S.C. Solar Photocatalysis for Water Disinfection: Materials and Reactor Design. *Catal. Sci. Technol.* **2014**, *4*, 1211–1226, https://doi.org/10.1039/C4CY00006D.
81. Filice, S.; D'Angelo, D.; Libertino, S.; Nicotera, I.; Kosma, V.; Privitera, V.; Scalese, S. Graphene Oxide and Titania Hybrid Nafion Membranes for Efficient Removal of Methyl Orange Dye from Water. *Carbon* **2015**, *C*, 489–499, https://doi.org/10.1016/j.carbon.2014.10.093.
82. Yew, S.-P.; Tang, H.-Y.; Sudesh, K. Photocatalytic Activity and Biodegradation of Polyhydroxybutyrate Films Containing Titanium Dioxide. *Polym. Degrad. Stab.* **2006**, *91*, 1800–1807, https://doi.org/10.1016/j.polymdegradstab.2005.11.011.
83. Cantarella, M.; Sanz, R.; Buccheri, M.A.; Ruffino, F.; Rappazzo, G.; Scalese, S.; Impellizzeri, G.; Romano, L.; Privitera, V. Immobilization of Nanomaterials in PMMA Composites for Photocatalytic Removal of Dyes, Phenols and Bacteria from Water. *J. Photochem. Photobiol. Chem.* **2016**, *321*, 1–11, https://doi.org/10.1016/j.jphotochem.2016.01.020.
84. Ding, Z.; Hu, X.; Lu, G.Q.; Yue, P.-L.; Greenfield, P.F. Novel Silica Gel Supported TiO2 Photocatalyst Synthesized by CVD Method. *Langmuir* **2000**, *16*, 6216–6222, https://doi.org/10.1021/la000119l.

85. Liu, X.; Ma, X.; Zhu, L.; Li, D. Photocatalysis, Microstructure, and Surface Characterization of TiO2-Loaded Wooden-Activated Carbon Fibers. *Polym. Compos.* **2015**, *36*, 62–68, https://doi.org/10.1002/pc.22913.
86. Iwasaki, M.; Miyamoto, Y.; Ito, S.; Furuzono, T.; Park, W.-K. Fabrication of Platy Apatite Nanocrystals Loaded with TiO2 Nanoparticles by Two-Step Emulsion Method and Their Photocatalytic Activity. *J. Colloid Interface Sci.* **2008**, *326*, 537–540, https://doi.org/10.1016/j.jcis.2008.07.041.
87. Zhou, D.; Ji, Z.; Jiang, X.; Dunphy, D.R.; Brinker, J.; Keller, A.A. Influence of material properties on TiO2 nanoparticle agglomeration. *PLoS One* **2013**, *8*, https://doi.org/10.1371/journal.pone.0081239.
88. Tasbihi, M.; Štangar, U.L.; Škapin, A.S.; Ristić, A.; Kaučič, V.; Tušar, N.N. Titania-Containing Mesoporous Silica Powders: Structural Properties and Photocatalytic Activity towards Isopropanol Degradation. *J. Photochem. Photobiol. Chem.* **2010**, *216*, 167–178, https://doi.org/10.1016/j.jphotochem.2010.07.011.
89. Okuno, T.; Kawamura, G.; Muto, H.; Matsuda, A. Photocatalytic Properties of Au-Deposited Mesoporous SiO2–TiO2 Photocatalyst under Simultaneous Irradiation of UV and Visible Light. *J. Solid State Chem.* **2016**, *235*, 132–138, https://doi.org/10.1016/j.jssc.2015.12.025.
90. Mahesh, K.P.O.; Kuo, D.-H.; Huang, B.-R. Facile Synthesis of Heterostructured Ag-Deposited SiO2@TiO2 Composite Spheres with Enhanced Catalytic Activity towards the Photodegradation of AB 1 Dye. *J. Mol. Catal. Chem.* **2015**, *396*, 290–296, https://doi.org/10.1016/j.molcata.2014.10.017.
91. Yu, L.; Yang, X.; Wang, D. TiO2 Incorporated in Magnetic Mesoporous SBA-15 by a Facile Inner-Pore Hydrolysis Process toward Enhanced Adsorption–Photocatalysis Performances for As(III). *J. Colloid Interface Sci.* **2015**, *448*, 525–532, https://doi.org/10.1016/j.jcis.2015.02.071.
92. Tseng, H.-H.; Lee, W.W.; Wei, M.-C.; Huang, B.-S.; Hsieh, M.-C.; Cheng, P.-Y. Synthesis of TiO2/SBA-15 Photocatalyst for the Azo Dye Decolorization through the Polyol Method. *Chem. Eng. J.* **2012**, *210*, 529–538, https://doi.org/10.1016/j.cej.2012.09.036.
93. Amar, A.H. Development of a Simple Dip Coating Method for Immobilization of TiO2 onto Solid Supports Using Direct TiO2 Powder. PhD Thesis, Ph. D Thesis, Universiti Sains Malaysia, Malaysia, **2007**.
94. Buchdahl, R. Mechanical properties of polymers and composites. *Journal of Polymer Science: Polymer Letters Edition* **1975**, *13*, 120-121, https://doi.org/10.1002/pol.1975.130130214..
95. Sutisna; Wibowo, E.; Rokhmat, M.; Rahman, D.Y.; Murniati, R.; Khairurrijal; Abdullah, M. Batik Wastewater Treatment Using TiO2 Nanoparticles Coated on the Surface of Plastic Sheet. *Procedia Eng.* **2017**, *170*, 78–83, https://doi.org/10.1016/j.proeng.2017.03.015.
96. Cámara, R.M.; Portela, R.; Gutiérrez-Martín, F.; Sánchez, B. Evaluation of Several Commercial Polymers as Support for TiO2 in Photo-Catalytic Applications. *GlobalNEST International Journal* **2014**, *16*, 525-535.
97. Ali, U.; Karim, K.J.B.A.; Buang, N.A. A Review of the Properties and Applications of Poly (Methyl Methacrylate) (PMMA). *Polym. Rev.* **2015**, *55*, 678–705, https://doi.org/10.1080/15583724.2015.1031377.
98. Dutschke, A.; Diegelmann, C.; Löbmann, P. Preparation of TiO2 Thin Films on Polystyrene by Liquid Phase Deposition. *J. Mater. Chem.* **2003**, *13*, 1058–1063, https://doi.org/10.1039/B212535H.
99. Tchoul, M.N.; Fillery, S.P.; Koerner, H.; Drummy, L.F.; Oyerokun, F.T.; Mirau, P.A.; Durstock, M.F.; Vaia, R.A. Assemblies of Titanium Dioxide-Polystyrene Hybrid Nanoparticles for Dielectric Applications. *Chem. Mater.* **2010**, *22*, 1749–1759, https://doi.org/10.1021/cm903182n.
100. Ye, C.; Li, H.; Cai, A.; Gao, Q.; Zeng, X. Preparation and Characterization of Organic Nano-Titanium Dioxide/Acrylate Composite Emulsions by in-Situ Emulsion Polymerization. *J. Macromol. Sci. Part A* **2011**, *48*, 309–314, https://doi.org/10.1080/10601325.2011.552353.
101. Mesnage, A.; Abdel Magied, M.; Simon, P.; Herlin-Boime, N.; Jégou, P.; Deniau, G.; Palacin, S. Grafting Polymers to Titania Nanoparticles by Radical Polymerization Initiated by Diazonium Salt. *J. Mater. Sci.* **2011**, *46*, 6332–6338, https://doi.org/10.1007/s10853-011-5709-z.
102. Lu, S.; Sun, S.-S.; Niu, J.; Zeng, L.; Liu, H.; Zhao, X. Poly (Thienylene Methine) Grafted Nanocrystalline TiO2 Based Hybrid Solar Cells. *J. Mater. Sci. Mater. Electron.* **2012**, *23*, 251–256, https://doi.org/10.1007/s10854-011-0397-7.
103. Essawy, A.A.; Ali, A.E.-H.; Abdel-Mottaleb, M.S.A. Application of Novel Copolymer-TiO2 Membranes for Some Textile Dyes Adsorptive Removal from Aqueous Solution and Photocatalytic Decolorization. *J. Hazard. Mater.* **2008**, *157*, 547–552, https://doi.org/10.1016/j.jhazmat.2008.01.072.
104. Pandey, N.; Khaling, R.; Verma, P.; Pendke, P.; Patel, A. Characterization of TiO2 Doped Poly (Methyl Methacrylate) PMMA Thin Films Using XRD. *AIP Conf. Proc.* **2019**, *2100*, https://doi.org/10.1063/1.5098705.
105. Benhabiles, O.; Galiano, F.; Marino, T.; Mahmoudi, H.; Lounici, H.; Figoli, A. Preparation and Characterization of TiO2-PVDF/PMMA Blend Membranes Using an Alternative Non-Toxic Solvent for UF/MF and Photocatalytic Application. *Molecules* **2019**, *24*, https://doi.org/10.3390/molecules24040724.
106. Graß, B.; Neyer, A.; Jöhnck, M.; Siepe, D.; Eisenbeiß, F.; Weber, G.; Hergenröder, R. A New PMMA-Microchip Device for Isotachophoresis with Integrated Conductivity Detector. *Sens. Actuators B Chem.* **2001**, *72*, 249–258, https://doi.org/10.1016/S0925-4005(00)00643-2.
107. Cheng, J.-Y.; Wei, C.-W.; Hsu, K.-H.; Young, T.-H. Direct-Write Laser Micromachining and Universal Surface Modification of PMMA for Device Development. *Sens. Actuators B Chem.* **2004**, *99*, 186–196, https://doi.org/10.1016/j.snb.2003.10.022.

108. Demir, M.M.; Castignolles, P.; Akbey, Ü.; Wegner, G. In-Situ Bulk Polymerization of Dilute Particle/MMA Dispersions. *Macromolecules* **2007**, *40*, 4190–4198, https://doi.org/10.1021/ma070142e.
109. Demir, M.M.; Memesa, M.; Castignolles, P.; Wegner, G. PMMA/Zinc Oxide Nanocomposites Prepared by In-Situ Bulk Polymerization. *Macromol. Rapid Commun.* **2006**, *27*, 763–770, https://doi.org/10.1002/marc.200500870.
110. Motaung, T.E.; Luyt, A.S.; Bondioli, F.; Messori, M.; Saladino, M.L.; Spinella, A.; Nasillo, G.; Caponetti, E. PMMA–Titania Nanocomposites: Properties and Thermal Degradation Behaviour. *Polym. Degrad. Stab.* **2012**, *97*, 1325–1333, https://doi.org/10.1016/j.polymdegradstab.2012.05.022.
111. Inkyo, M.; Tokunaga, Y.; Tahara, T.; Iwaki, T.; Iskandar, F.; Hogan, C.J.; Okuyama, K. Beads Mill-Assisted Synthesis of Poly Methyl Methacrylate (PMMA)-TiO2 Nanoparticle Composites. *Ind. Eng. Chem. Res.* **2008**, *47*, 2597–2604, https://doi.org/10.1021/ie071069j.
112. Chatterjee, A. Properties Improvement of PMMA Using Nano TiO2. *J. Appl. Polym. Sci.* **2010**, *118*, 2890–2897, https://doi.org/10.1002/app.32567.
113. Meng, X.; Zhang, Z.; Luo, N.; Cao, S.; Yang, M. Transparent poly(methyl methacrylate)/TiO2 nanocomposites for UV-shielding applications. *Polymer Science Series A* **2011**, *53*, 977, https://doi.org/10.1134/S0965545X11100099.
114. Zhao, R.; Chen, C.; Li, Q.; Luo, W. Effects of Stress and Physical Ageing on Nonlinear Creep Behavior of Poly(Methyl Methacrylate). *J. Cent. South Univ. Technol.* **2008**, *15*, 582–588, https://doi.org/10.1007/s11771-008-0426-8.
115. Ummartyotin, S.; Bunnak, N.; Juntaro, J.; Sain, M.; Manuspiya, H. Hybrid Organic–Inorganic of ZnS Embedded PVP Nanocomposite Film for Photoluminescent Application. *Comptes Rendus Phys.* **2012**, *13*, 994–1000, https://doi.org/10.1016/j.crhy.2012.09.008.
116. Ghosh, S.; Remita, H.; Basu, R.N. Visible-Light-Induced Reduction of Cr(VI) by PDPB-ZnO Nanohybrids and Its Photo-Electrochemical Response. *Appl. Catal. B Environ.* **2018**, *239*, 362–372, https://doi.org/10.1016/j.apcatb.2018.08.034.
117. Ghosh, S.; Kouamé, N.A.; Ramos, L.; Remita, S.; Dazzi, A.; Deniset-Besseau, A.; Beaunier, P.; Goubard, F.; Aubert, P.-H.; Remita, H. Conducting Polymer Nanostructures for Photocatalysis under Visible Light. *Nat. Mater.* **2015**, *14*, 505–511, https://doi.org/10.1038/nmat4220.
118. Ghosh, S.; Mallik, A.K.; Basu, R.N. Enhanced Photocatalytic Activity and Photoresponse of Poly(3,4-Ethylenedioxythiophene) Nanofibers Decorated with Gold Nanoparticle under Visible Light. *Sol. Energy* **2018**, *159*, 548–560, https://doi.org/10.1016/j.solener.2017.11.036.
119. He, J.-H.; Liu, Y.; Mo, L.-F.; Wan, Y.-Q.; Xu, L. *Electrospun nanofibres and their applications*. ISmithers Shawbury, UK: **2008**.
120. Li, Y.; Zhao, H.; Yang, M. TiO2 Nanoparticles Supported on PMMA Nanofibers for Photocatalytic Degradation of Methyl Orange. *J. Colloid Interface Sci.* **2017**, *508*, 500–507, https://doi.org/10.1016/j.jcis.2017.08.076.
121. Ramakrishna, S. *An Introduction to Electrospinning and Nanofibers*. World Scientific, **2005.**
122. Mondal, K.; Ali, Md.A.; Agrawal, V.V.; Malhotra, B.D.; Sharma, A. Highly Sensitive Biofunctionalized Mesoporous Electrospun TiO2 Nanofiber Based Interface for Biosensing. *ACS Appl. Mater. Interfaces* **2014**, *6*, 2516–2527, https://doi.org/10.1021/am404931f.
123. Ab Kadir, R.; Li, Z.; Sadek, A.Z.; Abdul Rani, R.; Zoolfakar, A.S.; Field, M.R.; Ou, J.Z.; Chrimes, A.F.; Kalantar-zadeh, K. Electrospun Granular Hollow SnO2 Nanofibers Hydrogen Gas Sensors Operating at Low Temperatures. *J. Phys. Chem. C* **2014**, *118*, 3129–3139, https://doi.org/10.1021/jp411552z.
124. Koysuren, O. Preparation and Characterization of Polyvinyl Alcohol/Carbon Nanotube (PVA/CNT) Conductive Nanofibers. *J. Polym. Eng.* **2012**, *32*, 407–413, https://doi.org/10.1515/polyeng-2012-0068.
125. Koysuren, O.; Karaman, M.; Dinc, H. Preparation and Characterization of Polyvinyl Borate/Polyvinyl Alcohol (PVB/PVA) Blend Nanofibers. *J. Appl. Polym. Sci.* **2012**, *124*, 2736–2741, https://doi.org/10.1002/app.35035.
126. Koysuren, O.; Karaman, M.; Yildiz, H.B.; Koysuren, H.N.; Dinc, H. Electrospun Polyvinyl Borate/Poly(Methyl Methacrylate) (PVB/PMMA) Blend Nanofibers. *Int. J. Polym. Mater. Polym. Biomater.* **2014**, *63*, 337–341, https://doi.org/10.1080/00914037.2013.845188.
127. Alipour, D.; Keshtkar, A.R.; Moosavian, M.A. Adsorption of Thorium(IV) from Simulated Radioactive Solutions Using a Novel Electrospun PVA/TiO2/ZnO Nanofiber Adsorbent Functionalized with Mercapto Groups: Study in Single and Multi-Component Systems. *Appl. Surf. Sci.* **2016**, *366*, 19–29, https://doi.org/10.1016/j.apsusc.2016.01.049.
128. Wanjale, S.; Birajdar, M.; Jog, J.; Neppalli, R.; Causin, V.; Karger-Kocsis, J.; Lee, J.; Panzade, P. Surface Tailored PS/TiO2 Composite Nanofiber Membrane for Copper Removal from Water. *J. Colloid Interface Sci.* **2016**, *469*, 31–37, https://doi.org/10.1016/j.jcis.2016.01.054.
129. Yagub, M.T.; Sen, T.K.; Afroze, S.; Ang, H.M. Dye and Its Removal from Aqueous Solution by Adsorption: A Review. *Adv. Colloid Interface Sci.* **2014**, *209*, 172–184, https://doi.org/10.1016/j.cis.2014.04.002.
130. Zaharia, C.; Suteu, D.; Muresan, A.; Muresan, R.; Popescu, A. Textile Wastewater Treatment by Homogenous Oxidation with Hydrogen Peroxide. *Environ. Eng. Manag. J.* **2009**, *8*, 1359–1369, https://doi.org/10.30638/eemj.2009.199.

131. Suteu, D.; Zaharia, C.; Măluțan, T. Biosorbents Based on Lignin Used in Biosorption Processes from Wastewater Treatment. A Review. In: *Lignin: Properties and Applications in Biotechnology and Bioenergy*. **2012**; pp. 278–305.
132. Chincholi, M.; Sagwekar, P.; Nagaria, C.; Kulkarni, S.; Dhokpande, S. Removal of Dye by Adsorption on Various Adsorbents: A Review. *Int J Sci Eng Technol Res* **2014**, *3*, 835–840.
133. Abrahart, E.N. *Dyes and Their Intermediates*. Edward Arnold, **1977**; https://doi.org/10.1016/0160-9327%2877%2990195-8.
134. Welham, A. The Theory of Dyeing (and the Secret of Life). *J. Soc. Dye. Colour.* **2000**, *116*, 140–143.
135. Rothenberg, M. *History of Science in United States. An Encyclopedia*. 1st edition, New York, 2000; https://doi.org/10.4324/9780203902806.
136. Humans, I.W. IARC monographs on the evaluation of carcinogenic risks to humans. Ingested nitrate and nitrite, and cyanobacterial peptide toxins. *IARC monographs on the evaluation of carcinogenic risks to humans* **2010**, *94*.
137. Saravanan, R.; Shankar, H.; Prakash, T.; Narayanan, V.; Stephen, A. ZnO/CdO Composite Nanorods for Photocatalytic Degradation of Methylene Blue under Visible Light. *Mater. Chem. Phys.* **2011**, *125*, 277–280, https://doi.org/10.1016/j.matchemphys.2010.09.030.
138. Clarke, E.A.; Anliker, R. Organic Dyes and Pigments. Anthropogenic Compounds. In: *The Handbook of Environmental Chemistry*. Anliker, R.; Butler, G.C.; Clarke, E.A.; Förstner, U.; Funke, W.; Hyslop, C.; Kaiser, G.; Rappe, C.; Russow, J.; Tölg, G.; Zander, M.; Zitko, V. Eds.; Springer: Berlin, Heidelberg, **1980**; pp. 181–215.
139. Hunger, K. *Industrial Dyes: Chemistry, Properties, Applications*. John Wiley & Sons, **2007**.
140. Zollinger, H. *Color Chemistry: Syntheses, Properties, and Applications of Organic Dyes and Pigments*. John Wiley & Sons, **2003**; https://doi.org/10.1002/anie.200385122.
141. Mishra, G.; Tripathy, M. A Critical Review of the Treatment for Decolorization of Dye Wastewater. *Colourage* **1993**, *40*, 35–38, https://doi.org/10.1016/j.ecoenv.2021.113160.
142. Demirbas, A. Agricultural Based Activated Carbons for the Removal of Dyes from Aqueous Solutions: A Review. *J. Hazard. Mater.* **2009**, *167*, 1–9, https://doi.org/10.1016/j.jhazmat.2008.12.114.
143. Robinson, T.; McMullan, G.; Marchant, R.; Nigam, P. Remediation of Dyes in Textile Effluent: A Critical Review on Current Treatment Technologies with a Proposed Alternative. *Bioresour. Technol.* **2001**, *77*, 247–255, https://doi.org/10.1016/S0960-8524(00)00080-8.
144. Walthall, W.K.; Stark, J.D. The Acute and Chronic Toxicity of Two Xanthene Dyes, Fluorescein Sodium Salt and Phloxine B, to Daphnia Pulex. *Environ. Pollut.* **1999**, *104*, 207–215, https://doi.org/10.1016/S0269-7491(98)00189-4.
145. Tsuda, S.; Murakami, M.; Matsusaka, N.; Kano, K.; Taniguchi, K.; Sasaki, Y.F. DNA Damage Induced by Red Food Dyes Orally Administered to Pregnant and Male Mice. *Toxicol. Sci. Off. J. Soc. Toxicol.* **2001**, *61*, 92–99, https://doi.org/10.1093/toxsci/61.1.92.
146. Chiou, M.-S.; Ho, P.-Y.; Li, H.-Y. Adsorption of Anionic Dyes in Acid Solutions Using Chemically Cross-Linked Chitosan Beads. *Dyes Pigments* **2004**, *60*, 69–84, https://doi.org/10.1016/S0143-7208(03)00140-2.
147. González, J.A.; Villanueva, M.E.; Piehl, L.L.; Copello, G.J. Development of a Chitin/Graphene Oxide Hybrid Composite for the Removal of Pollutant Dyes: Adsorption and Desorption Study. *Chem. Eng. J.* **2015**, *280*, 41–48, https://doi.org/10.1016/j.cej.2015.05.112.
148. Laing, D.; Kean, W.F. The Greening Of Healthcare: Fabrics Used In Health Care Facilities. *J. Green Build.* **2011**, *6*, 45–64, https://doi.org/10.3992/jgb.6.4.45.
149. Maron, D.M.; Ames, B.N. Revised Methods for the Salmonella Mutagenicity Test. *Mutat. Res. Mutagen. Relat. Subj.* **1983**, *113*, 173–215, https://doi.org/10.1016/0165-1161(83)90010-9.
150. Tünay, O.; Kabdasli, I.; Eremektar, G.; Orhon, D. Color Removal from Textile Wastewaters. *Water Sci. Technol.* **1996**, *34*, 9–16, https://doi.org/10.1016/S0273-1223(96)00815-3.
151. Mall, I.D.; Srivastava, V.C.; Agarwal, N.K.; Mishra, I.M. Adsorptive removal of malachite green dye from aqueous solution by bagasse fly ash and activated carbon-kinetic study and equilibrium isotherm analyses. *Colloids and Surfaces A: Physicochemical and Engineering Aspects* **2005**, *264*, 17-28, https://doi.org/10.1016/j.colsurfa.2005.03.027.
152. Shaul, G.M.; Holdsworth, T.J.; Dempsey, C.R.; Dostal, K.A. Fate of Water Soluble Azo Dyes in the Activated Sludge Process. *Chemosphere* **1991**, *22*, 107–119, https://doi.org/10.1016/0045-6535(91)90269-J.
153. Peters, R.J.B.; van Bemmel, G.; Herrera-Rivera, Z.; Helsper, H.P.F.G.; Marvin, H.J.P.; Weigel, S.; Tromp, P.C.; Oomen, A.G.; Rietveld, A.G.; Bouwmeester, H. Characterization of Titanium Dioxide Nanoparticles in Food Products: Analytical Methods to Define Nanoparticles. *J. Agric. Food Chem.* **2014**, *62*, 6285–6293, https://doi.org/10.1021/jf5011885.
154. Brittain, H.G.; Barbera, G.; DeVincentis, J.; Newman, A.W. Titanium Dioxide. In: *Analytical Profiles of Drug Substances and Excipients*. Brittain, H.G. Ed.; Academic Press: **1992**; Volume 21, pp. 659-691, https://doi.org/10.1016/S0099-5428(08)60404-9.
155. Shi, H.; Magaye, R.; Castranova, V.; Zhao, J. Titanium dioxide nanoparticles: a review of current toxicological data. *Particle and Fibre Toxicology* **2013**, *10*, https://doi.org/10.1186/1743-8977-10-15.

156. Hwu, Y.; Yao, Y.D.; Cheng, N.F.; Tung, C.Y.; Lin, H.M. X-Ray Absorption of Nanocrystal TiO2. *Nanostructured Mater.* **1997**, *9*, 355–358, https://doi.org/10.1016/S0965-9773(97)00082-2.
157. Demina, P.; Zybinskii, A.; Kuz'micheva, G.; Obolenskaya, L.; Savinkina, E.; Prokudina, N. Adsorption Ability of Samples with Nanoscale Anatase to Extract Nb(V) and Ta(V) Ions from Aqueous Media. *Crystallogr. Rep.* **2014**, *59*, 430–436, https://doi.org/10.1134/S1063774514030079.
158. Addamo, M.; Bellardita, M.; Paola, A.D.; Palmisano, L. Preparation and Photoactivity of Nanostructured Anatase, Rutile and Brookite TiO2 Thin Films. *Chem. Commun.* **2006**, 4943–4945, https://doi.org/10.1039/B612172A.
159. Andersson, S.; Wadsley, A.D. Crystallographic shear and diffusion paths in certain higher oxides of niobium, tungsten, molybdenum and titanium. *Nature* **1966**, *211*, 581-583, https://doi.org/10.1038/211581a0.
160. Kandiel, T.A.; Feldhoff, A.; Robben, L.; Dillert, R.; Bahnemann, D.W. Tailored Titanium Dioxide Nanomaterials: Anatase Nanoparticles and Brookite Nanorods as Highly Active Photocatalysts. *Chemistry of Materials* **2010**, *22*, 2050-2060, https://doi.org/10.1021/cm903472p.
161. Diebold, U. Chapter 11 - The Structure of TiO2 Surfaces. In: *The Chemical Physics of Solid Surfaces. Oxide Surfaces.* Woodruff, D.P. Ed.; Elsevier, **2001**; Volume 9, pp. 443–484.
162. Hebenstreit, E.L.D.; Hebenstreit, W.; Geisler, H.; Ventrice, C.A.; Hite, D.A.; Sprunger, P.T.; Diebold, U. The Adsorption of Chlorine on TiO2(110) Studied with Scanning Tunneling Microscopy and Photoemission Spectroscopy. *Surf. Sci.* **2002**, *505*, 336–348, https://doi.org/10.1016/S0039-6028(02)01385-7.
163. Finnegan, M.P.; Zhang, H.; Banfield, J.F. Phase Stability and Transformation in Titania Nanoparticles in Aqueous Solutions Dominated by Surface Energy. *The Journal of Physical Chemistry C* **2007**, *111*, 1962-1968, https://doi.org/10.1021/jp063822c.
164. Samat, M.H.; Ali, A.M.M.; Taib, M.F.M.; Hassan, O.H.; Yahya, M.Z.A. Hubbard U calculations on optical properties of 3d transition metal oxide TiO2. *Results in Physics* **2016**, *6*, 891-896, https://doi.org/10.1016/j.rinp.2016.11.006.
165. Stepanov, A.; Xiao, X.; Ren, F. Implantation of Titanium Dioxide with Transition Metalions. In: *Titanium Dioxide: Applications, Synthesis and Toxicity*. Prafulla, K.J. Nova Science Publishers, Inc.Editors: **2013**; pp. 59–83.
166. Sclafani, A.; Herrmann, J.M. Comparison of the Photoelectronic and Photocatalytic Activities of Various Anatase and Rutile Forms of Titania in Pure Liquid Organic Phases and in Aqueous Solutions. *J. Phys. Chem.* **1996**, *100*, 13655–13661, https://doi.org/10.1021/jp9533584.
167. Sakai, N.; Ebina, Y.; Takada, K.; Sasaki, T. Electronic Band Structure of Titania Semiconductor Nanosheets Revealed by Electrochemical and Photoelectrochemical Studies. *J. Am. Chem. Soc.* **2004**, *126*, 5851–5858, https://doi.org/10.1021/ja0394582.
168. Fujishima, F. TiO_2 Photocatalysis Fundamentals and Applications. *Revolut. Clean. Technol.* **1999**, 14–21.
169. Mo, S.-D.; Ching, W.Y. Electronic and Optical Properties of Three Phases of Titanium Dioxide: Rutile, Anatase, and Brookite. *Phys. Rev. B* **1995**, *51*, 13023–13032, https://doi.org/10.1103/PhysRevB.51.13023.
170. Le, H.A.; Linh, L.T.; Chin, S.; Jurng, J. Photocatalytic degradation of methylene blue by a combination of TiO2-anatase and coconut shell activated carbon. *Powder Technology* **2012**, *225*, 167-175, https://doi.org/10.1016/j.powtec.2012.04.004.
171. He, Z.; Que, W.W.X.; Xie, H. Titanium Dioxide: Synthesis and Toxicity of TiO2 Nanostructures. In: *Titanium Dioxide: Applications, Synthesis and Toxicity*. **2013**; pp. 37–58.
172. Chen, D.; Zhu, Q.; Lv, Z.; Deng, X.; Zhou, F.; Deng, Y. Microstructural and Photocatatlytic Properties of Eu-Doped Mesporous Titanium Dioxide Nanopaticles by Sol–Gel Method. *Mater. Res. Bull.* **2012**, *47*, 3129–3134, https://doi.org/10.1016/j.materresbull.2012.08.021.
173. Toygun, Ş.; Köneçoğlu, G.; Kalpaklı, Y. General Principles of Sol-Gel. *Sigma* **2013**, *31*, 456–476.
174. Sun, M.; Zhang, X.; Li, J.; Cui, X.; Sun, D.; Lin, Y. Thermal Formation of Silicon-Doped TiO2 Thin Films with Enhanced Visible Light Photoelectrochemical Response. *Electrochem. Commun.* **2012**, *16*, 26–29, https://doi.org/10.1016/j.elecom.2011.12.015.
175. Lee, H.; Song, M.Y.; Jurng, J.; Park, Y.-K. The synthesis and coating process of TiO2 nanoparticles using CVD process. *Powder Technology* **2011**, *214*, 64-68, https://doi.org/10.1016/j.powtec.2011.07.036.
176. Nyankson, E.; Agyei-Tuffour, B.; Asare, J.; Annan, E.; Rwenyagila, E.R.; Konadu, D.S.; Yaya, A.; Dodoo-Arhin, D. Nanostructured TiO2 and Their Energy Applications-a Review. *Energy* **2013**.
177. Khataee, A.; Mansoori, G.A. *Nanostructured Titanium Dioxide Materials: Properties, Preparation and Applications*. World Scientific, **2011**; https://doi.org/10.1142/8325.
178. Halary-Wagner, E.; Bret, T.; Hoffmann, P. Light-Induced CVD of Titanium Dioxide Thin Films I: Kinetics of Deposition. *Chem. Vap. Depos.* **2005**, *11*, 21–28, https://doi.org/10.1002/cvde.200306303.
179. Li, D.; Bulou, S.; Gautier, N.; Elisabeth, S.; Goullet, A.; Richard-Plouet, M.; Choquet, P.; Granier, A. Nanostructure and Photocatalytic Properties of TiO2 Films Deposited at Low Temperature by Pulsed PECVD. *Appl. Surf. Sci.* **2019**, *466*, 63–69, https://doi.org/10.1016/j.apsusc.2018.09.230.
180. Arifin, P.; Mustajab, M.A.; Haryono, S.; Adhika, D.R.; Nugraha, A.A. MOCVD Growth and Characterization of TiO2 Thin Films for Hydrogen Gas Sensor Application. *Mater. Res. Express* **2019**, *6*, https://doi.org/10.1088/2053-1591/ab192b.

181. Wang, F.; Zhu, N.; Li, T.; Zhang, H.-C. Material and Energy Efficiency Analysis of Low Pressure Chemical Vapor Deposition of TiO2 Film. *Procedia CIRP* **2014**, *15*, 32–37, https://doi.org/10.1016/j.procir.2014.06.044.
182. Zhang, M.; Jin, Z.; Zhang, J.; Guo, X.; Yang, J.; Li, W.; Wang, X.; Zhang, Z. Effect of Annealing Temperature on Morphology, Structure and Photocatalytic Behavior of Nanotubed H2Ti2O4(OH)2. *J. Mol. Catal. Chem.* **2004**, *217*, 203–210, https://doi.org/10.1016/j.molcata.2004.03.032.
183. Tsai, C.-C.; Nian, J.-N.; Teng, H. Mesoporous Nanotube Aggregates Obtained from Hydrothermally Treating TiO2 with NaOH. *Appl. Surf. Sci.* **2006**, *253*, 1898–1902, https://doi.org/10.1016/j.apsusc.2006.03.035.
184. Kolen'ko, Yu.V.; Churagulov, B.R.; Kunst, M.; Mazerolles, L.; Colbeau-Justin, C. Photocatalytic Properties of Titania Powders Prepared by Hydrothermal Method. *Appl. Catal. B Environ.* **2004**, *54*, 51–58, https://doi.org/10.1016/j.apcatb.2004.06.006.
185. Thapa, R.; Maiti, S.; Rana, T.H.; Maiti, U.N.; Chattopadhyay, K.K. Anatase TiO2 Nanoparticles Synthesis via Simple Hydrothermal Route: Degradation of Orange II, Methyl Orange and Rhodamine B. *J. Mol. Catal. Chem.* **2012**, *363–364*, 223–229, https://doi.org/10.1016/j.molcata.2012.06.013.
186. Donar, Y.O.; Bilge, S.; Sınağ, A.; Pliekhov, O. TiO2/Carbon Materials Derived from Hydrothermal Carbonization of Waste Biomass: A Highly Efficient, Low-Cost Visible-Light-Driven Photocatalyst. *ChemCatChem* **2018**, *10*, 1134–1139, https://doi.org/10.1002/cctc.201701405.
187. Malik, M.A.; Wani, M.Y.; Hashim, M.A. Microemulsion Method: A Novel Route to Synthesize Organic and Inorganic Nanomaterials: 1st Nano Update. *Arab. J. Chem.* **2012**, *5*, 397–417, https://doi.org/10.1016/j.arabjc.2010.09.027.
188. Anuratha, K.S.; Peng, H.-S.; Xiao, Y.; Su, T.-S.; Wei, T.-C.; Lin, J.-Y. Electrodeposition of Nanostructured TiO2 Thin Film as an Efficient Bifunctional Layer for Perovskite Solar Cells. *Electrochimica Acta* **2019**, *295*, 662–667, https://doi.org/10.1016/j.electacta.2018.10.181.
189. Su, T.-S.; Hsieh, T.-Y.; Hong, C.-Y.; Wei, T.-C. Electrodeposited Ultrathin TiO2 Blocking Layers for Efficient Perovskite Solar Cells. *Sci. Rep.* **2015**, *5*, 16098, https://doi.org/10.1038/srep16098.
190. Dikici, T.; Yurddaşkal, M. Anodik spark oksitleme tekniği ile üretilen titanyum dioksit (TiO2) kaplamaların karakterizasyonu ve fotokatalitik özellikleri. *Balıkesir Üniversitesi Fen Bilim. Enstitüsü Derg.* **2018**, *20*, 83–93, https://doi.org/10.25092/baunfbed.427766.
191. Sul, Y.-T.; Johansson, C.B.; Jeong, Y.; Albrektsson, T. The Electrochemical Oxide Growth Behaviour on Titanium in Acid and Alkaline Electrolytes. *Med. Eng. Phys.* **2001**, *23*, 329–346, https://doi.org/10.1016/S1350-4533(01)00050-9.
192. Diamanti, M.V.; Pedeferri, M.P. Effect of Anodic Oxidation Parameters on the Titanium Oxides Formation. *Corros. Sci.* **2007**, *49*, 939–948, https://doi.org/10.1016/j.corsci.2006.04.002.
193. Diamanti, M.V.; Ormellese, M.; Pedeferri, M. Application-Wise Nanostructuring of Anodic Films on Titanium: A Review. *J. Exp. Nanosci.* **2015**, *10*, 1285–1308, https://doi.org/10.1080/17458080.2014.999261.
194. Fries, R.; Simkó, M. (Nano-)Titanium dioxide (Part I): Basics, Production, Applications. *ISBN* **2013**, https://doi.org/10.1553/ita-nt-033en.
195. Kallio, T.; Alajoki, S.; Pore, V.; Ritala, M.; Laine, J.; Leskelä, M.; Stenius, P. Antifouling Properties of TiO2: Photocatalytic Decomposition and Adhesion of Fatty and Rosin Acids, Sterols and Lipophilic Wood Extractives. *Colloids Surf. Physicochem. Eng. Asp.* **2006**, *291*, 162–176, https://doi.org/10.1016/j.colsurfa.2006.06.044.
196. Nwanya, A.; Ezema, F.; Ejikeme, P. Dyed Sensitized Solar Cells: A Technically and Economically Alternative Concept to p-n Junction Photovoltaic Devices. *Int. J. Phys. Sci.* **2011**, *6*, 5190–5201.
197. Bharathi, J.J.; Pappayee, N. Titanium Dioxide (TiO2) Thin Film Based Gas Sensors. *J Chem Pharm Sci* **2014**, *4*, 59–61.
198. Khataee, A.R.; Kasiri, M.B. Photocatalytic Degradation of Organic Dyes in the Presence of Nanostructured Titanium Dioxide: Influence of the Chemical Structure of Dyes. *J. Mol. Catal. Chem.* **2010**, *328*, 8–26, https://doi.org/10.1016/j.molcata.2010.05.023.
199. Skocaj, M.; Filipic, M.; Petkovic, J.; Novak, S. Titanium Dioxide in Our Everyday Life; Is It Safe? *Radiol. Oncol.* **2011**, *45*, 227–247, https://doi.org/10.2478/v10019-011-0037-0.
200. Youkhana, E.Q.; Feltis, B.; Blencowe, A.; Geso, M. Titanium Dioxide Nanoparticles as Radiosensitisers: An In Vitro and Phantom-Based Study. *Int. J. Med. Sci.* **2017**, *14*, 602–614, https://doi.org/10.7150/ijms.19058.
201. Stoilova, O.; Manolova, N.; Rashkov, I. Electrospun Poly(Methyl Methacrylate)/TiO2 Composites for Photocatalytic Water Treatment. *Polymers* **2021**, *13*, https://doi.org/10.3390/polym13223923.
202. Mills, A.; Le Hunte, S. An Overview of Semiconductor Photocatalysis. *J. Photochem. Photobiol. Chem.* **1997**, *108*, 1–35, https://doi.org/10.1016/S1010-6030(97)00118-4.
203. Herrmann, J.-M. Heterogeneous photocatalysis: fundamentals and applications to the removal of various types of aqueous pollutants. *Catalysis Today* **1999**, *53*, 115-129, https://doi.org/10.1016/S0920-5861(99)00107-8.

204. Herrmann, J.-M.; Mozzanega, M.-N.; Pichat, P. Oxidation of Oxalic Acid in Aqueous Suspensions of Semiconductors Illuminated with UV or Visible Light. *J. Photochem.* **1983**, *22*, 333–343, https://doi.org/10.1016/0047-2670(83)85012-6.
205. Herrmann, J.M.; Guillard, C.; Arguello, M.; Agüera, A.; Tejedor, A.; Piedra, L.; Fernández-Alba, A. Photocatalytic Degradation of Pesticide Pirimiphos-Methyl: Determination of the Reaction Pathway and Identification of Intermediate Products by Various Analytical Methods. *Catal. Today* **1999**, *54*, 353–367, https://doi.org/10.1016/S0920-5861(99)00196-0.
206. Qamar, M.; Gondal, M.A.; Yamani, Z.H. Synthesis of Highly Active Nanocrystalline WO3 and Its Application in Laser-Induced Photocatalytic Removal of a Dye from Water. *Catal. Commun.* **2009**, *10*, 1980–1984, https://doi.org/10.1016/j.catcom.2009.07.014.
207. Feng, S.; Zhao, J.; Zhu, Z. Kinetically Restraining Aggregation of ZnS Nanocrystals and the Effect on Photocatalysis. *Mater. Sci. Eng. B* **2008**, *150*, 116–120, https://doi.org/10.1016/j.mseb.2008.02.002.
208. Neppolian, B.; Sakthivel, S.; Arabindoo, B.; Palanichamy, M.; Murugesan, V. Degradation of Textile Dye by Solar Light Using TiO2 and ZnO Photocatalysts. *J. Environ. Sci. Health Part A* **1999**, *34*, 1829–1838, https://doi.org/10.1080/10934529909376931.
209. Devipriya, S.P.; Yesodharan, S. Photocatalytic degradation of phenol in water using TiO2 and ZnO. *Journal of environmental biology* **2010**, *31*, 247-249.
210. Haider, A.J.; Alhaddad, R.M.S.; Yahya, K.Z. Nanostructure Dopants TiO2 Films for Gas Sensing. *Iraqi J. Appl. Phys.* **2011**, *7*, 27-31.
211. Nyamukamba, P. Preparation of Photocatalytic TiO_2 Nanoparticles Immobilized on Carbon Nanofibres for Water Purification. University Of Fort Hare **2011**.
212. Matsunaga, T.; Tomoda, R.; Nakajima, T.; Wake, H. Photoelectrochemical Sterilization of Microbial Cells by Semiconductor Powders. *FEMS Microbiol. Lett.* **1985**, *29*, 211–214, https://doi.org/10.1111/j.1574-6968.1985.tb00864.x.
213. Kotani, Y.; Matoda, T.; Matsuda, A.; Kogure, T.; Tatsumisago, M.; Minami, T. Anatase Nanocrystal-Dispersed Thin Films via Sol–Gel Process with Hot Water Treatment: Effects of Poly(Ethylene Glycol) Addition on Photocatalytic Activities of the Films. *J. Mater. Chem.* **2001**, *11*, 2045–2048, https://doi.org/10.1039/B103043B.
214. Cho, S.; Choi, W. Solid-Phase Photocatalytic Degradation of PVC–TiO2 Polymer Composites. *J. Photochem. Photobiol. Chem.* **2001**, *143*, 221–228, https://doi.org/10.1016/S1010-6030(01)00499-3.
215. Linsebigler, A.L.; Lu, G.; Yates, J.T. Photocatalysis on TiO2 Surfaces: Principles, Mechanisms, and Selected Results. *Chem. Rev.* **1995**, *95*, 735–758, https://doi.org/10.1021/cr00035a013.
216. Al-Rasheed, R.A. Water treatment by heterogeneous photocatalysis an overview. **2005**; pp. 1-14.
217. Herrmann, J.-M. Heterogeneous Photocatalysis: State of the Art and Present Applications In Honor of Pr. R.L. Burwell Jr. (1912–2003), Former Head of Ipatieff Laboratories, Northwestern University, Evanston (Ill). *Top. Catal.* **2005**, *34*, 49–65, https://doi.org/10.1007/s11244-005-3788-2.
218. Poulios, I.; Tsachpinis, I. Photodegradation of the Textile Dye Reactive Black 5 in the Presence of Semiconducting Oxides. *J. Chem. Technol. Biotechnol.* **1999**, *74*, 349–357, https://doi.org/10.1002/(SICI)1097-4660(199904)74:4<349::AID-JCTB5>3.0.CO;2-7.
219. Piscopo, A.; Robert, D.; Weber, J.V. Influence of PH and Chloride Anion on the Photocatalytic Degradation of Organic Compounds: Part I. Effect on the Benzamide and Para-Hydroxybenzoic Acid in TiO2 Aqueous Solution. *Appl. Catal. B Environ.* **2001**, *35*, 117–124, https://doi.org/10.1016/S0926-3373(01)00244-2.
220. Wong, M.S.; Sun, D.S.; Chang, H.H. Bactericidal performance of visible-light responsive titania photocatalyst with silver nanostructures. *PLoS One* **2010**, *5*, https://doi.org/10.1371/journal.pone.0010394.
221. Foster, H.A.; Ditta, I.B.; Varghese, S.; Steele, A. Photocatalytic disinfection using titanium dioxide: spectrum and mechanism of antimicrobial activity. *Appl Microbiol Biotechnol* **2011**, *90*, 1847-1868, https://doi.org/10.1007/s00253-011-3213-7.
222. Utami, F.D.; Rahman, D.Y.; Sustini, E.; Abdullah, M. Immobilization of TiO2 on Transparent Plastic and Its Application in Photocatalytic Wastewater Treatment. *J. Phys.: Conf. Ser.* **2019**, *1171*, https://doi.org/10.1088/1742-6596/1171/1/012030.
223. Ray, C.; Pal, T. Retracted Article: Recent Advances of Metal–Metal Oxide Nanocomposites and Their Tailored Nanostructures in Numerous Catalytic Applications. *J. Mater. Chem. A* **2017**, *5*, 9465–9487, https://doi.org/10.1039/C7TA02116J.
224. Alamgir, M.; Nayak, G.C.; Mallick, A.; Tiwari, S.K.; Mondal, S.; Gupta, M. Processing of PMMA Nanocomposites Containing Biocompatible GO and TiO2 Nanoparticles. *Mater. Manuf. Process.* **2018**, *33*, 1291–1298, https://doi.org/10.1080/10426914.2018.1424996.
225. Sul, O.; Kim, K.; Choi, E.; Kil, J.; Park, W.; Lee, S.-B. Reduction of Hole Doping of Chemical Vapor Deposition Grown Graphene by Photoresist Selection and Thermal Treatment. *Nanotechnology* **2016**, *27*, https://doi.org/10.1088/0957-4484/27/50/505205.
226. Deng, C.; Lin, W.; Agnus, G.; Dragoe, D.; Pierucci, D.; Ouerghi, A.; Eimer, S.; Barisic, I.; Ravelosona, D.; Chappert, C.; Zhao, W. Reversible Charge-Transfer Doping in Graphene due to Reaction with Polymer Residues. *The Journal of Physical Chemistry C* **2014**, *118*, 13890-13897, https://doi.org/10.1021/jp501077t.

227. Giti, R.; Zomorodian, K.; Firouzmandi, M.; Zareshahrabadi, Z.; Rahmannasab, S. Antimicrobial Activity of Thermocycled Polymethyl Methacrylate Resin Reinforced with Titanium Dioxide and Copper Oxide Nanoparticles. *Int. J. Dent.* **2021**, *2021*, https://doi.org/10.1155/2021/6690806.
228. An, H. Improving Tensile Strength of Polymer Blends as Prosthetic Foot MaterialReinforcement by Carbon Fiber. *J. Mater. Sci. Eng.* **2015**, *4*, 1–3, https://doi.org/10.4172/2169-0022.1000158.
229. Anžlovar, A.; Crnjak Orel, Z.; Kogej, K.; ¦igon, M. Polyol-Mediated Synthesis of Zinc Oxide Nanorods and Nanocomposites with Poly(methyl methacrylate). *Journal of Nanomaterials* **2012**, *2012*, https://doi.org/10.1155/2012/760872.
230. Liang, B.; Tang, S.; Jiang, Q.; Chen, C.; Chen, X.; Li, S.; Yan, X. Preparation and characterization of PEO-PMMA polymer composite electrolytes doped with nano-Al2O3. *Electrochimica Acta* **2015**, *169*, 334-341, https://doi.org/10.1016/j.electacta.2015.04.039.
231. Li, Y.; Wang, Z.; Zhao, H.; Yang, M. Composite of TiO2 Nanoparticles and Carbon Nanotubes Loaded on Poly(Methyl Methacrylate) Nanofibers: Preparation and Photocatalytic Performance. *Synth. Met.* **2020**, *269*, https://doi.org/10.1016/j.synthmet.2020.116529.
232. Xie, Y.; Sun, X.-F.; Li, W.; He, J.; Sun, R.; Hu, S.; Wu, Y. Fabrication of Electrospun Xylan-g-PMMA/TiO2 Nanofibers and Photocatalytic Degradation of Methylene Blue. *Polymers* **2022**, *14*, https://doi.org/10.3390/polym14122489.
233. Zhuo, Y.; Liu, J.; Wang, Y.; Li, Q.; Xu, X.; Ren, X. Preparation and Photocatalytic Property of Electrospun Nano-TiO2/Poly(Methylmethacrylate) Nanofibres. *Ferroelectrics* **2019**, *548*, 143–149, https://doi.org/10.1080/00150193.2019.1592521.
234. Li, Y.; Zhao, H.; Yang, M. TiO2 nanoparticles supported on PMMA nanofibers for photocatalytic degradation of methyl orange. *Journal of Colloid and Interface Science* **2017**, *508*, 500-507, https://doi.org/10.1016/j.jcis.2017.08.076.
235. Zhang, Y.; Cai, W.; Xie, C.; Wu, H. Visible-light-responsive γ-Fe2O3/PMMA/S-TiO2 core/shell nanocomposite: Preparation, characterization and photocatalytic activity. *Materials Science in Semiconductor Processing* **2016**, *48*, 45-51, https://doi.org/10.1016/j.mssp.2016.02.023.
236. Kaijun, Z.; Qingshan, L.; Yu, W. Preparation and performance of PMMA/R-TiO2 and PMMA/A-TiO2 electrospun fibrous films. *Integrated Ferroelectrics* **2018**, *188*, 31-43, https://doi.org/10.1080/10584587.2018.1454760.
237. Cantarella, M.; Sanz, R.; Buccheri, M.A.; Romano, L.; Privitera, V. PMMA/TiO2 nanotubes composites for photocatalytic removal of organic compounds and bacteria from water. *Materials Science in Semiconductor Processing* **2016**, *42*, 58-61, https://doi.org/10.1016/j.mssp.2015.07.053.
238. Klaysri, R.; Preechawan, V.; Thammachai, N.; Praserthdam, P.; Mekasuwandumrong, O. Photocatalytic activity of Nitrogen and Silica doping on TiO2 nanocatalyst and grafted onto PMMA film. *Materials Chemistry and Physics* **2018**, *211*, 420-427, https://doi.org/10.1016/j.matchemphys.2018.02.049.
239. Koysuren, O.; Koysuren, H.N. Photocatalytic activities of poly(methyl methacrylate)/titanium dioxide nanofiber mat. *Journal of Macromolecular Science, Part A* **2017**, *54*, 80-84, https://doi.org/10.1080/10601325.2017.1261619.
240. Li, Y.; Wang, Z.; Zhao, H.; Huang, X.; Yang, M. 3D MoS2@TiO2@poly(methyl methacrylate) nanocomposite with enhanced photocatalytic activity. *Journal of Colloid and Interface Science* **2019**, *557*, 709-721, https://doi.org/10.1016/j.jcis.2019.09.074.